nature communications

Article

https://doi.org/10.1038/s41467-024-52793-6

Sol-moiety: Discovery of a water-soluble prodrug technology for enhanced oral bioavailability of insoluble therapeutics

Received: 23 February 2024

Accepted: 23 September 2024

Published online: 01 October 2024

Check for updates

Arvin B. Karbasi[1], Jaden D. Barfuss[1,4], Theodore C. Morgan[1,4], Daniel Collins[1], Drew A. Costenbader[1], David G. Dennis[1], Andrew Hinman[1], KyuWeon Ko[1], Cynthia Messina[1,2], Khanh C. Nguyen[3], Rebecca C. Schugar[2], Karin A. Stein[1], Brianna B. Williams[1], Haixia Xu[2], Justin P. Annes[2] & Mark Smith[1]

Though conceptually attractive, the use of water-soluble prodrug technology to enhance oral bioavailability of highly insoluble small molecule therapeutics has not been widely adopted. In large part, this is due to the rapid enzymatic or chemical hydrolysis of prodrugs within the gastrointestinal tract, resulting in drug precipitation and no overall improvement in oral bioavailability relative to standard formulation strategies. We reasoned that an optimal water-soluble prodrug could be attained if the rate of prodrug hydrolysis were reduced to favor drug absorption rather than drug precipitation. In doing so, the rate of hydrolysis provides a pharmacokinetic control point for drug delivery. Herein, we report the discovery of a water-soluble promoiety (Sol-moiety) technology to optimize the oral bioavailability of highly insoluble small molecule therapeutics, possessing various functional groups, without the need for sophisticated, often toxic, lipid or organic solvent-based formulations. The power of the technology is demonstrated with marked pharmacokinetic improvement of the commercial drugs enzalutamide, vemurafenib, and paclitaxel. This led to a successful efficacy study of a water-soluble orally administered prodrug of paclitaxel in a mouse pancreatic tumor model.

Despite holding much promise, relatively few solubilizing prodrugs have been developed to enhance the oral bioavailability of therapeutics with poor aqueous solubility. The majority of these prodrugs consist of a phosphate or phosphonooxymethyl moiety, as the increase in ionic character enhances aqueous solubility (Fig. 1a)[1–6]. Several more water-soluble prodrugs have been developed for intravenous administration; again, largely using phosphate or phosphonooxymethyl groups (Fig. 1b)[7–15]. Clinically approved alternatives to the use of phosphates and phosphonooxymethyl are limited to the succinic acid formyl ester prodrug, used to improve the solubility of the anti-malarial drug artesunate[16], a bis-piperidinyl carbamate group, found to enhance the solubility of the intravenously administered topoisomerase inhibitor irinotecan[17], and ethyl methyl(pyridin-2-yl) carbamate, found on antimalarial drug, isovuconazonium sulfate[18].

There are several reasons why solubilizing prodrugs for oral delivery have not been widely adopted by the pharmaceutical industry, these include the complexities associated with chemical synthesis, poor selection of drug substrate, compound stability, and varying solubilities at the different pH levels encountered following drug consumption[19–22]. Still, the major drawback of current solubilizing

[1]Sarafan ChEM-H, Stanford University, Stanford, CA 94305, USA. [2]Division of Endocrinology, Stanford University School of Medicine, Stanford, CA 94305, USA. [3]Division of Gastroenterology and Hepatology, Stanford University School of Medicine, Stanford, CA 94305, USA. [4]These authors contributed equally: Jaden D. Barfuss, Theodore C. Morgan. e-mail: mxsmith@stanford.edu

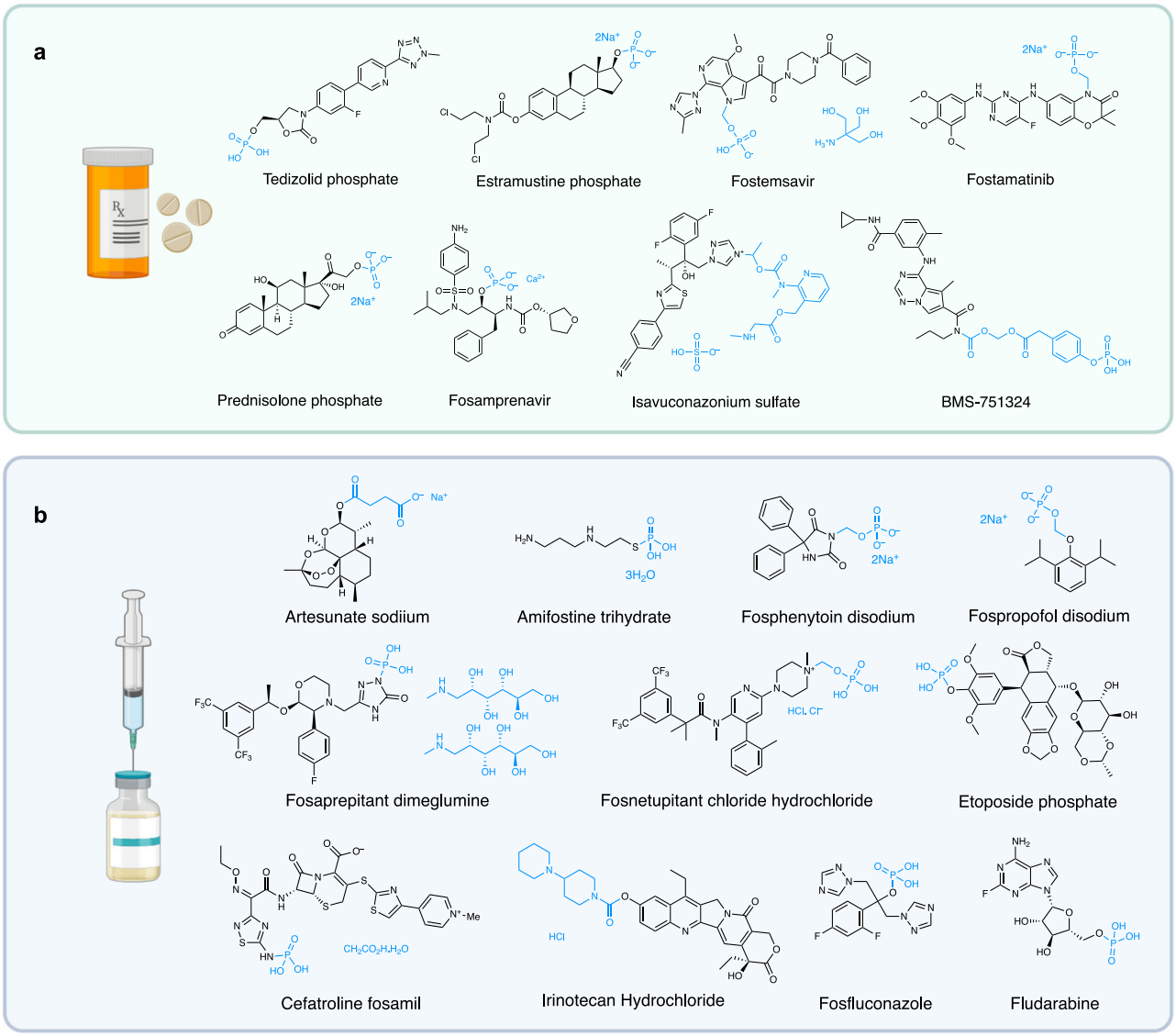

Fig. 1 | Examples of water-soluble prodrugs. a Orally administered therapeutics that possess a water-soluble promoiety (e.g. phosphate or phosphonooxymethyl group). **b** Intravenously administered commercial drugs possessing various water-soluble promoieties. Created in BioRender. Smith, M. (2024) BioRender.com/l22c048.

prodrug technology is the rapid precipitation of the released drug in the stomach or small intestine upon chemical or enzymatic hydrolysis, resulting in no overall improvement in the rate or extent of absorption[21–24]. One of the few examples where this stability concern has been successfully addressed was in the development of the P38α MAP kinase inhibitor, BMS-751324 (Fig. 1a)[25]. Herein, a 4-(phosphonooxy)phenylacetate moiety was linked to the parent drug through a carbamate methylene ester. This compound was found to be stable at both pH 1.2 and 6.5 but requires hydrolysis from both alkaline phosphatases and carboxylesterases for drug release and has not been widely adopted.

High solubility throughout the varying pH levels of the gastrointestinal tract is essential for therapeutics to be readily absorbed into the bloodstream. However, the majority of small molecule therapeutics tend to be lipophilic and poorly soluble in water. In preclinical settings, dimethyl sulfoxide (DMSO) or polyethylene glycol (PEG)-based formulations are commonplace for rodent pharmacokinetic (PK) or pharmacodynamic (PD) studies. However, the data generated can often mislead people into thinking a compound is developable, only to encounter varying oral bioavailability or dose proportionality once in clinical development. To address these concerns, sophisticated formulation strategies including particle size reduction, surfactants, co-solvents, amorphous solid dispersions, and lipid nanoparticles are often relied upon to improve compound dissolution and bioavailability[26,27]. However, such approaches are often time-consuming[28], expensive, and does not necessarily provide sufficient drug exposure to observe efficacy in a clinical setting.

In this work, we report the design, synthesis and biological evaluation of a water-soluble prodrug technology that addresses the aforementioned concerns and enables the pharmacokinetic optimization of drug prototypes in a timely manner without the need for formulation development.

Results

The design hypothesis of Sol-moiety

To overcome the limitations of current solubilizing prodrug technology, we conceived of a solubilizing promoiety (Sol-moiety) approach where drug solubility and stability could be maintained throughout the physiologically encountered pH levels of the gastrointestinal tract[19,20] Ideally, the rate of enzymatic conversion in the intestine could be titrated, so that the rate of absorption is greater than the rate of precipitation of the released therapeutic. To test this hypothesis, we

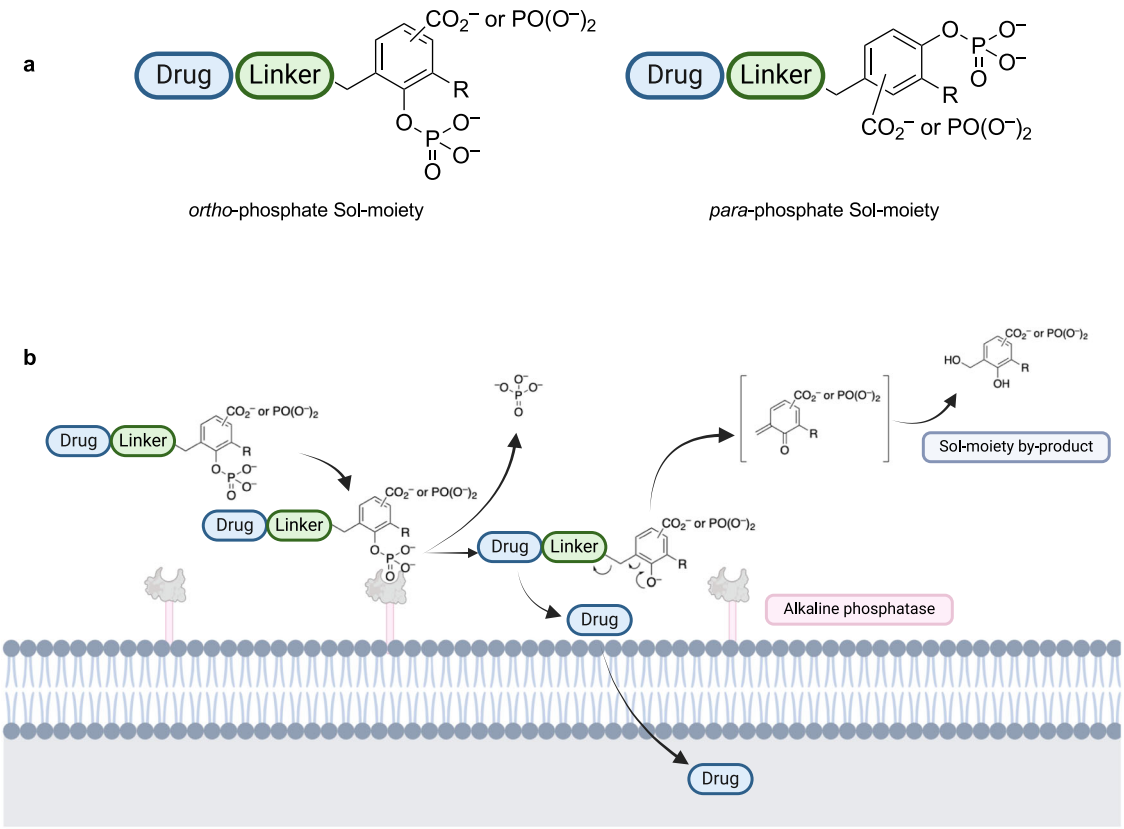

Fig. 2 | Schematic of the Sol-moiety concept. a Generic example of the solubilizing promoiety (Sol-moiety) prototypes. The phosphate group can be located in either the *ortho*- or *para*-positions to enable either 1,4 or 1,6-elimination to occur upon hydrolysis. **b** The Sol-moiety is enzymatically cleaved by alkaline phosphatases located on the apical side of the epithelial cells facing the gut lumen. The released drug is allowed to cross the cell membrane, whereas the released quinone methide is expected to be rapidly hydrolyzed to its 2-hydroxybenzyl alcohol derivative. Created in BioRender. Smith, M. (2024) BioRender.com/m87n291.

designed our Sol-moiety to consist of a benzyl scaffold substituted with a phosphate group in either the *ortho* or *para*-position, and either a carboxylate or phosphonate group (Fig. 2a). Drug liberation occurs by hydrolysis of the phosphate group by alkaline phosphatases located on the apical membrane of epithelial cells of the intestine, followed by a 1,4- or 1,6-elimination reaction (Fig. 2b). The addition of a carboxylate or phosphonate group enhances the ionic character of the molecule, ensuring solubility of the Sol-moiety drug-conjugate through the varying physiological pH's levels encountered in the gastrointestinal tract. Following drug release, the ionic character of the quinone methide, or its hydrolyzed benzyl alcohol derivative (Sol-moiety by-product), is expected to have poor membrane permeability, reducing potential toxicity concerns. Our design allows for control of the rate of enzymatic conversion by intestinal alkaline phosphatases with substituents that could alter the steric and/or electronic environment surrounding the phosphate group, similar to previously published observations on fluorogenic substrates using the alkaline phosphatase, PTP1B[29]. Sol-moiety can be attached to a drug directly or through various linkers such as a formyl or carbonyl group, to enabling the elimination reaction to occur following hydrolysis of the phosphate group. For this study, we made the arbitrary decision to connect the phosphate group at the *ortho*-position (Fig. 2a).

In vitro studies to confirm Sol-moiety stability and cleavage

For initial screening, the Sol-moiety-drug conjugates **1**–**8** (Fig. 3) were synthesized and determined to be stable in both simulated gastric fluid (SGF) at pH 1.2 and Hank's balanced salt solution (HBSS) at pH 6.5 ($t_{1/2}$ = > 120 min) (Supplementary Table 1). All the compounds were shown to be substrates for hydrolysis in a human placental alkaline phosphatase assay that measured hydrolysis of the Sol-moiety-drug conjugate and the rate of formation of the parent drug (Fig. 4a and Supplementary Table 3). Next, the Sol-moiety-drug conjugates **1**–**8** were evaluated in the Caco-2 assay, which is known to display similar levels of alkaline phosphatases as that found in the human intestine due to its derivation from human colorectal adenocarcinoma cancer cells[22,30]. As expected, when the Sol-moiety-drug conjugates **1**–**8** were applied to the apical side of Caco-2 cells, no cell absorption was observed (Fig. 4ai) and only released drug was measured in the basolateral chamber (Fig. 4aii). The Sol-moiety by-products **9** and **10** were poorly absorbed, if at all (P_{app} = 0.1 and 0.0 × 10^{-6} cm/s respectively), supporting our theory that these would display limited permeability and potentially avoid any in vivo toxicity concerns that a hydroxybenzyl alcohol might possess.

In vivo pharmacokinetic studies

In a mouse cassette pharmacokinetic (PK) study, Sol-moiety prototypes (**1i, 2i, 3ii, 4i, 5i, 6i, 7ii**, and **8i**) were dosed via oral gavage using saline solution as the vehicle. Despite known limitations of cassette studies, due to potential inhibition of transporters and metabolizing enzymes, good exposure of released drug was observed for Sol-enzalutamide **1i** (AUC = 212.7 μM•hr), Sol-vemurafenib **2i** (AUC = 74.7 μM•hr), and Sol-desloratadine **7ii** (AUC = 217.5 μM•hr). Moderate or low exposure was observed for Sol-dabrafenib **3ii** (AUC = 0.08 μM•hr), Sol-apixaban **4i** (AUC = 2.75 μM•hr), Sol-carvedilol **5i** (AUC = 0.87 μM•hr), Sol-lenalidomide **6i** (AUC = 1.61 μM•hr) and Sol-paclitaxel **8i** (AUC = 0.27 μM•hr) (Fig. 4b). These data confirm our hypothesis that Sol-moiety-drug conjugates can be dosed via oral gavage in saline solution and provide good exposure levels, potentially replacing standard organic solvent-based formulations, such as DMSO or PEG, for highly water-insoluble preclinical compounds.

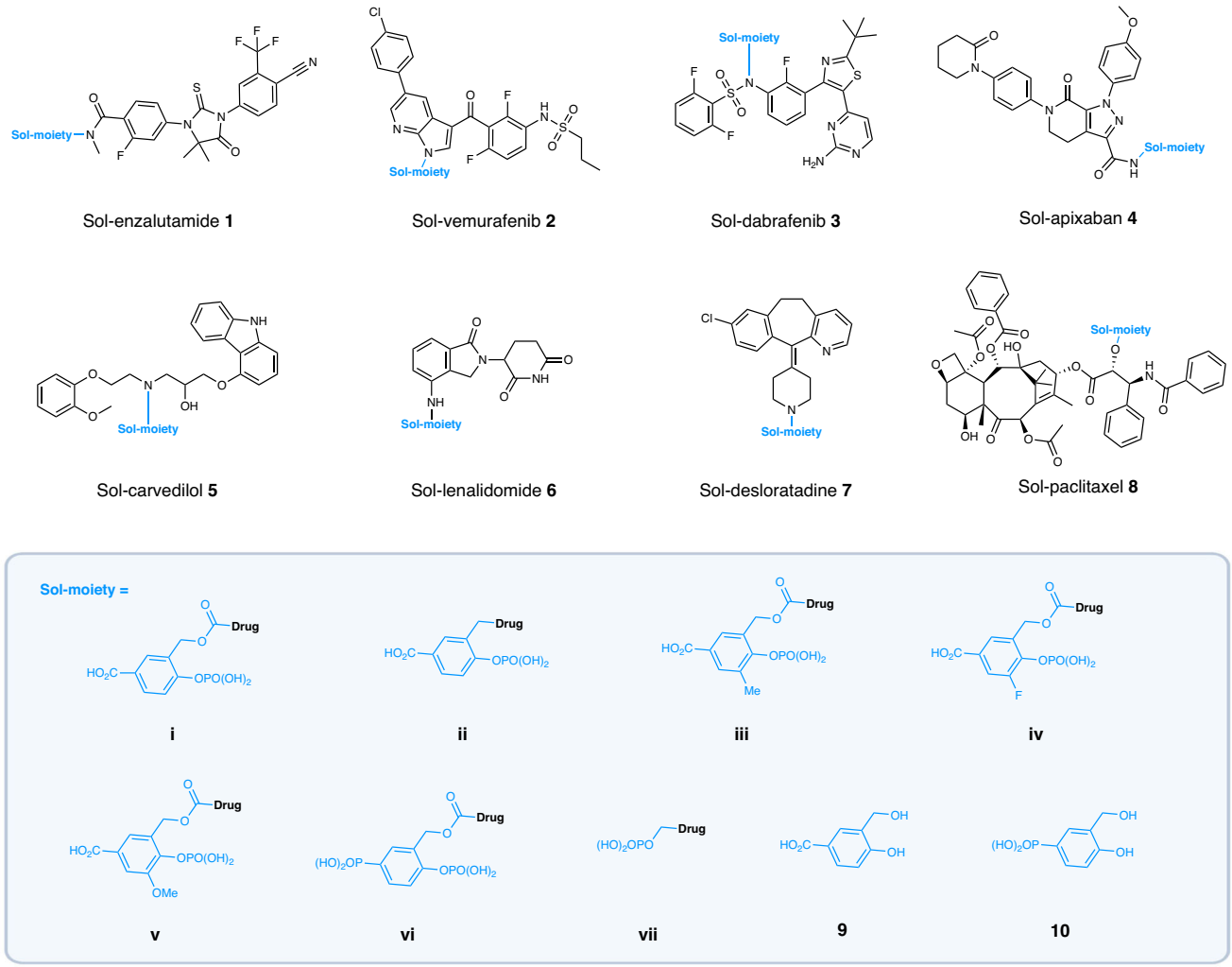

Fig. 3 | Structures of the Sol-moiety drug-conjugates used in the study. The solubilizing promoieties are colored in blue as well as the proposed major Sol-moiety by-products **9** and **10**. Background image created in BioRender. Smith, M. (2024) BioRender.com/z93c726.

Given the promising oral bioavailability observed for enzalutamide from the cassette PK study, we chose to directly compare the PK profiles of Sol-enzalutamide **1i** (formulated in water) to enzalutamide formulated in carboxymethylcellulose (CMC)/Tween 80[31]. Both compounds were dosed via oral gavage at 0.0215 mmol/kg and 0.107 mmol/kg (10 mg/kg and 50 mg/kg equivalent of enzalutamide) respectively. Enzalutamide was found to have an oral bioavailability of 45% at the 0.0215 mmol/kg dose, that decreased to 33% upon dose escalation. In contrast, Sol-enzalutamide **1i** displayed oral bioavailability of 64% at both dose levels, suggesting that solubility is potentially driving the lack of dose-proportional increase in exposure observed with the standard CMC formulation of enzalutamide (Fig. 5). Thus, at the 50 mg/kg dose equivalent of enzalutamide, a ~ 50% improvement in oral bioavailability was achieved using the water-based Sol-moiety technology. Next, attention focused on modifying the electronic and/or steric bulk around the phosphate group, to see if reducing the Sol-moiety hydrolysis rate could enhance the exposure of enzalutamide. Sol-enzalutamide analogs **1iii**–**v** were evaluated in the human placental alkaline phosphatase stability assay. Herein, a decrease in the rate of alkaline phosphatase hydrolysis was observed in accordance with the increase in steric bulk around the phosphate group (Fig. 6). The compounds (**1iii**–**v**) were then dosed at 0.0107 mmol/kg (5 mg/kg equivalent of enzalutamide), via oral gavage in a mouse PK experiment. Unfortunately, enzalutamide drug levels remained high at the 24-hour timepoint, so we were unable to clearly distinguish the differences in the oral bioavailability between the Sol-moiety analogs. However, an extended mouse PK study (72 h) with the methyl analog **1iii** at a dose of 0.021 mmol/kg (equivalent to a dose of 10 mg/kg enzalutamide) gave an AUC_{0-72} of 2133 μM•h that is equivalent to 86% oral bioavailability of enzalutamide (Fig. 5b), a notable improvement relative to **1i** (64% F) and almost a 2-fold boost in bioavailability over the standard CMC formulation of enzalutamide at the same dose. This supports our hypothesis that modifying steric and/or electronic substituents on the Sol-moiety modulates the rate of phosphate hydrolysis and, consequently, oral bioavailability of the released drug.

Encouraged by these results, we then investigated the highly insoluble and poorly permeable (BCS Class IV) BRAF mutant inhibitor, vemurafenib. When Sol-vemurafenib **2i** and **2vi** were dosed at 0.051 mmol/kg (25 mg/kg equivalent of vemurafenib), 96% and 113% oral bioavailability was observed, significantly higher (> 10-fold) than a 25 mg/kg dose of vemurafenib, formulated using PEG 400 with vitamin E (emulsifier) in saline. Once again, the concentrations of vemurafenib in plasma at 24 h, following delivery with Sol-vemurafenib **2i** and **2vi**, remained high, preventing pharmacokinetic differences between the two Sol-vemurafenib analogs from being fully distinguishable (Fig. 7). Interestingly, the Sol-vemurafenib analogs **2i** and **2vi** displayed elongated T_{max} and $t_{1/2}$ relative to vemurafenib, suggesting non-linear kinetics. Regardless, the results demonstrate the pharmacokinetic benefits of the water-soluble Sol-moiety technology over a standard PEG-based formulation and confirmed vemurafenib to be readily absorbed into mouse plasma once soluble.

https://doi.org/10.1038/s41467-024-52793-6

a

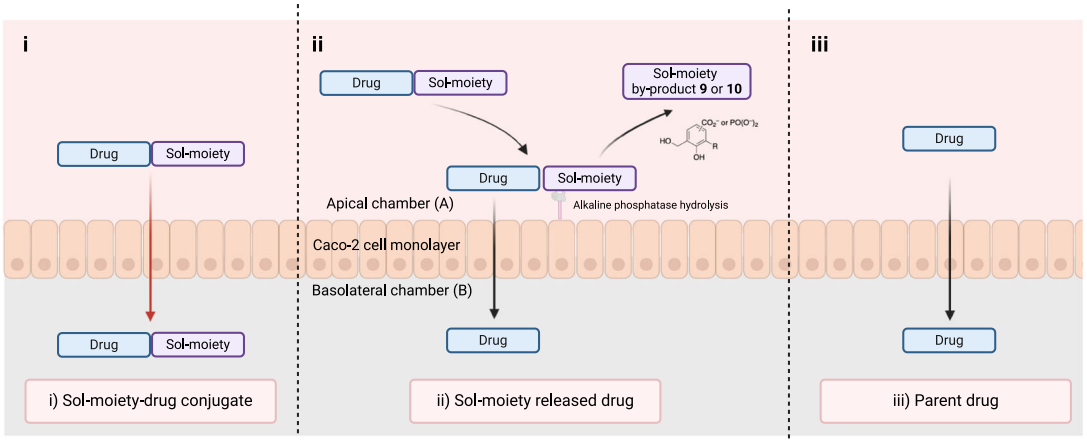

	1i	2i	3ii	4i	5i	6i	7ii	8i	9	10
i) Sol-moiety-drug conjugate P_{app} × 1e-6 cm/s (A–B)	0.0	0.0	0.0	0.0	0.0	0.0	0.0	0.0	–	–
ii) Sol-moiety released drug P_{app} × 1e-6 cm/s (A–B)	11.9	0.5	0.02	1.3	3.0	0.3	0.9	0.6	–	–
iii) (Parent) Drug P_{app} × 1e-6 cm/s (A–B)	20.1	1.4	12.4	3.0	7.6	1.2	5.9	1.1	0.1	0.0
Hydrolysis rate in ALP (pmol/min)[a]	4.16	0.64	1.26	1.65	2.11	2.24	1.53	2.13	–	–

[a]Assay performed using human placental alkaline phosphatase. Rate was determined on product formation.

b

	1i	2i	3ii	4i	5i	6i	7ii	8i	9	10
Mouse pharmacokinetic study oral dose (mmol/kg)	0.0107	0.0107	0.0107	0.0108	0.0128	0.019	0.0107	0.0041	0.024	0.122
Cmax (μM)	11.5	8.6	0.02	1.34	0.20	1.89	11.4	0.08	6.05	ND
AUC_{last} (μM•hr)$_{0–24\ h}$	212.7	74.7	0.08	2.75	0.87	1.61	217.5	0.27	3.93	ND

ND = Not detected in plasma samples

c

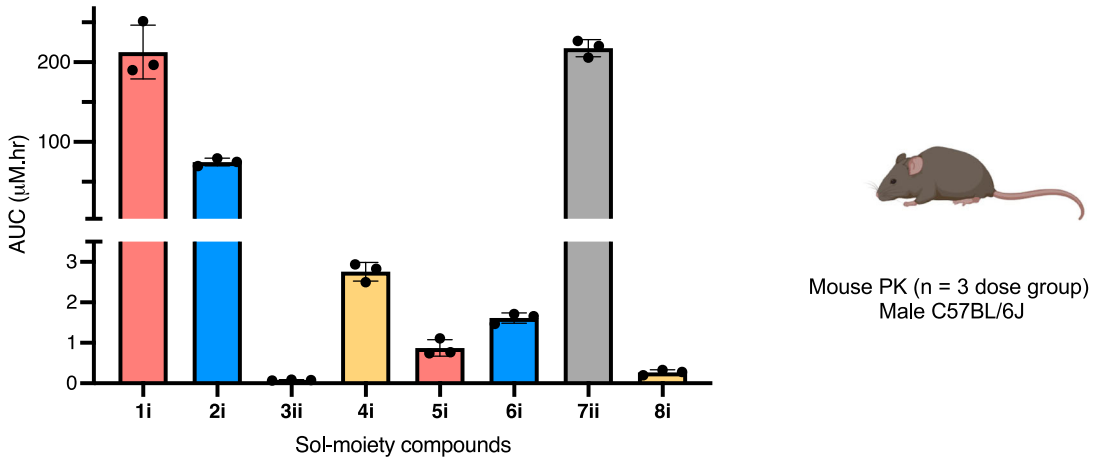

Fig. 4 | In vitro ADME and in vivo pharmacokinetic data for Sol-moiety drug-conjugates. a Comparison of caco−2 experiments to measure i) Permeability of Sol-moiety-drug conjugate; ii) Permeability of the released drug from Sol-moiety; and iii) the permeability of the parent drug (Papp A to B) measured in a separate experiment. The permeability of the Sol-moiety by products **9** and **10** were also measured as well as the hydrolysis rate using human placental alkaline phosphatase. Image created in BioRender. Smith, M. (2024) BioRender.com/x11n290. **b** Comparison of mouse PK AUC's of the Sol-moiety drug conjugates **1i, 2i, 3ii, 4i, 5i, 6i, 7ii, 8i** and Sol-moiety by-products **9** and **10**. Mouse PK experiments were cassette-dosed in saline solution. Appearance of parent drug or Sol-moiety by-product was monitored in mouse plasma with collections at various timepoints over 24 h. **c** Bar chart to highlight the AUC values for the parent drug following administration of the Sol-moiety drug conjugates **1i, 2i, 3ii, 4i, 5i, 6i, 7ii**, and **8i**. *n* = 3 mice per dose group. Data are presented as mean values +/− SD. Mouse image Created in BioRender. Smith, M. (2024) BioRender.com/y69d862.

https://doi.org/10.1038/s41467-024-52793-6

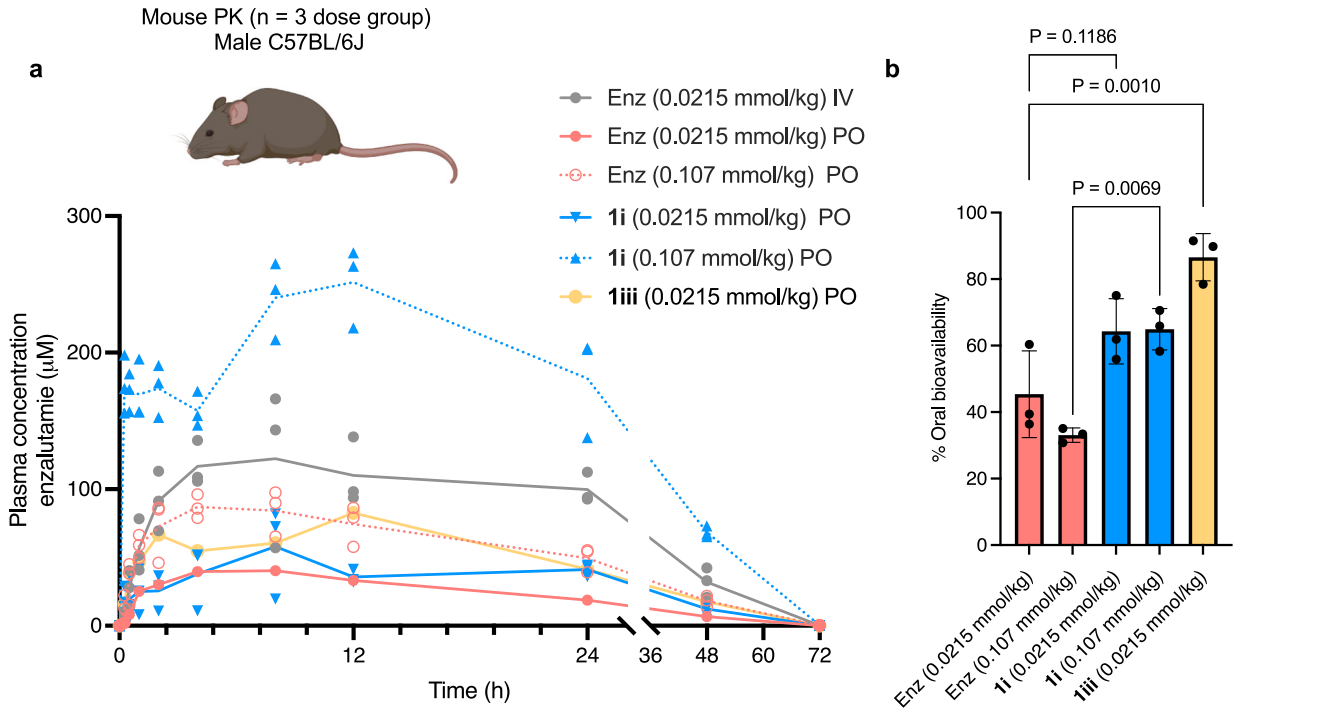

	Enzalutamide (Enz)			1i		1iii
Dose (mg/kg)	10	10	50	16.9 (10 mg/kg equivalent Enz)	86.4 (50 mg/kg equivalent Enz)	17.25 (10 mg/kg equivalent Enz)
Dose (mmol/kg)	0.0215	0.0215	0.107	0.0215	0.107	0.0215
Formulation	10% DMSO	CMC/Tween 80	CMC/Tween 80	Water	Water	Water
Route of administration	I.V.[a]	Oral	Oral	Oral	Oral	Oral
Cmax (μM)	91.1	47.3	149.3	66.3	267.2	76.3
Tmax (hr)	6.6	6.6	9.3	13.3	10.6	10.6
AUC (μM•hr) $_{0–72\ h}$	2470	1121	4093	1589	8023	2133

[a]Retro-orbital injection.

Fig. 5 | Comparison of mouse pharmacokinetic data of enzalutamide. a Plasma concentrations of enzalutamide were measured over a 72-hour time course. Enzalutamide was dosed intravenously using a standard DMSO-based formulation and orally using a carboxymethylcellulose/Tween 80 suspension, and PO dosing of Sol-enzalutamide **1i** and **1iii** was performed using deionized water as a vehicle. $n = 3$ mice per dose group. Line data represents mean values at each time point. Individual values per mice are shown. **b** Bar chart to show the difference in oral bioavailability observed for enzalutamide comparing a standard formulation and delivery due to Sol-enzalutamide **1i** and **1iii**. $n = 3$ mice per dose group. Data are presented as mean values +/− SD. Statistical significance determined using an ordinary one-way ANOVA with Tukey's multiple comparison test. Mouse image Created in BioRender. Smith, M. (2024) BioRender.com/y69d862.

Finally, we evaluated the impact of Sol-moiety technology on the oral bioavailability of the tubulin inhibitor, paclitaxel. Paclitaxel is a widely used chemotherapeutic that is highly insoluble in water and poorly absorbed (BCS Class IV), due to first-pass metabolism and efflux; consequently, it is intravenously administered to patients using Cremophor® EL as a formulation vehicle. As we had shown earlier, Sol-paclitaxel **8i** gave low to modest oral bioavailability following a dose of 0.004 mmol/kg (equivalent to 3.5 mg/kg of paclitaxel) (Fig. 4). However, we observed that **8i** was not particularly soluble (0.1 mg/mL) in its free acid form at pH 6.5 in HBSS. Therefore, to enhance solubility, the Sol-paclitaxel derivative **8vi** was prepared and found to be soluble at >49 mg/mL in HBSS also in its free acid form. Dosed orally to mice, at 0.004 mmol/kg (3.5 mg/kg equivalent of paclitaxel), **8vi** displayed a significant improvement in exposure (AUC = 0.98 μM•hr) with bioavailability of ~36%, a > 3-fold increase relative to **8i** and a 7-fold improvement over the previously described phosphonooxymethyl prodrug of paclitaxel **8vii** (Fig. 8)[32]. The rate of hydrolysis for **8vi** was also slightly lower (1.44 pmol/min) than **8i** (2.13 pmol/min) and **8vii** (2.03 pmol/min) (Supplementary Table 3). Although a slight decrease in dose proportionality was observed when **8vi** was administered by oral gavage in mice at 25 mg/kg and 75 mg/kg (18 and 55 mg/kg equivalent of paclitaxel) (Fig. 8), the overall oral bioavailability of **8vi** remained between 5–7-fold higher than **8vii** and clearly demonstrates superiority of the Sol-moiety technology over traditional water-soluble prodrugs.

In vivo pharmacodynamic study of Sol-paclitaxel 8vi

As the 75 mg/kg dose of Sol-paclitaxel (**8vi**) provided paclitaxel plasma concentrations over an extended time above the 0.05 μmol C_{trough} levels needed for in vivo efficacy[33], we conducted a proof-of-concept study using a BxPC-3 xenograft mouse model for pancreatic cancer, following a similar protocol described for a lipid-based formulation of oral paclitaxel[34]. The experiment was conducted using a vehicle arm (saline solution), a paclitaxel positive control dosed IV at 12.5 mg/kg

https://doi.org/10.1038/s41467-024-52793-6

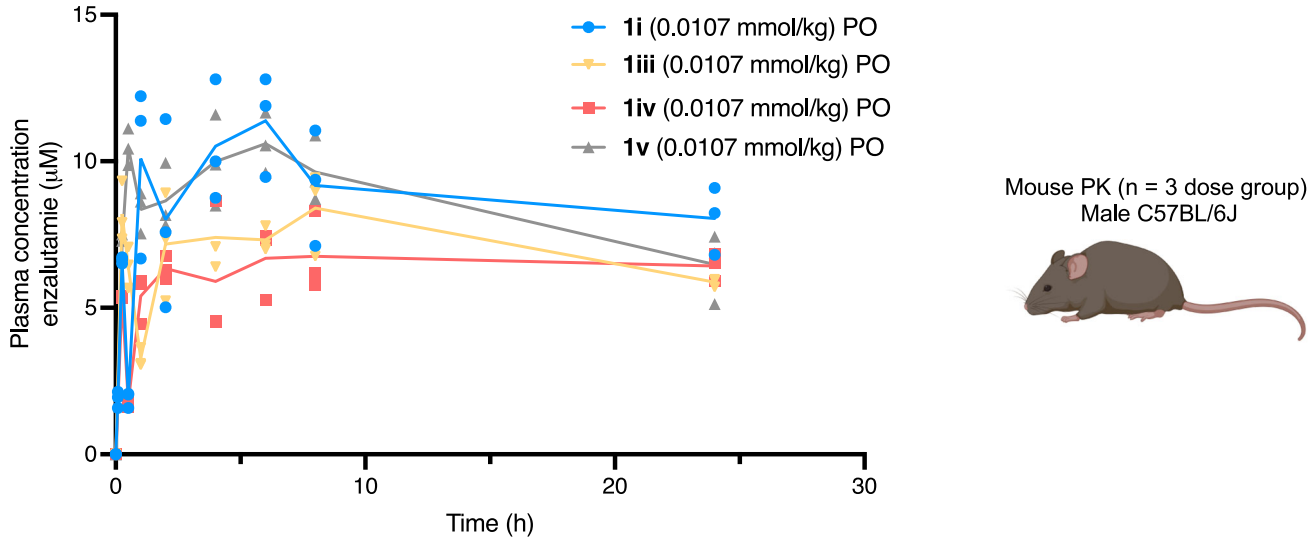

	1i[b]	1iii	1iv	1v
Hydrolysis rates in ALP solution (pmol/min)[a]	4.16	2.97	3.43	1.81
Caco-2 P_{app} × 1e-6 cm/s (AB)	0.0	0.0	0.0	0.0
Caco-2 P_{app} × 1e-6 cm/s (AB) enzalutamide	11.9	8.9	9.5	8.4
Dose (mg/kg)	8.8	8.8	8.8	8.9
Dose mmol/kg	0.0107	0.0107	0.0107	0.0107
Cmax (μM)	11.51	9.25	8.14	11.23
Tmax (hr)	3.67	5.42	6.0	3.5
AUC (μM•hr)$_{0–24\ h}$	212.7	170	153	204

[a]Human placental alkaline phosphatase. [b]Data previously shown in Table 4

Fig. 6 | Comparison of alkaline phosphatase, Caco-2 and mouse pharmacokinetic data using the Sol-moiety-drug conjugates 1i, 1iii, 1iv and 1 v. Compounds were dosed at an equivalent of 5 mg/kg of enzalutamide in saline solution and plasma concentrations measured over 24 h. $n = 3$ mice per dose group. Line data represents mean values at each time point. Mouse image Created in BioRender. Smith, M. (2024) BioRender.com/y69d862.

once a week (QWK) in Cremophor® EL, and Sol-paclitaxel **8vi** dosed PO at 25 mg/kg and 75 mg/kg every other day (QOD) in saline solution. Dosing was performed over 21 days and tumor growth monitored for an additional 25 days. Tumor volume and animal weight were monitored on a biweekly basis (Fig. 9a, b). Following the dosing period, the tumor growth inhibition (TGI) of the 25 mg/kg QOD dose of **8vi** was −15%, whereas the 75 mg/kg (55 mg/kg equivalent of paclitaxel) dose had a TGI of 91% that reduced to 84% following the 25-day observation period. The IV dose of 12.5 mg/kg paclitaxel had a TGI of 78% following the dosing period that reduced to 51% following the observation period. There was no appreciable toxicity reported during the dosing of Sol-paclitaxel **8vi**. Tumor and plasma concentrations of paclitaxel, measured at 6 and 24 h post-dose of **8vi**, confirmed reasonable dose-proportional exposure of paclitaxel. Interestingly, accumulation of paclitaxel in the tumor was observed at both doses of **8vi** after 24 h, with the 75 mg/kg dose being almost 10-fold higher than the desired trough level for efficacy (Fig. 9c). This is the first reported efficacy study using an orally bioavailable prodrug of paclitaxel and highlights the ability of the Sol-moiety technology to transform the route of drug administration from intravenous to oral.

In vivo exposure of the major sol-moiety by-products 9 and 10

Compound **9** was detected in mouse plasma following an oral dose of 4 mg/kg (AUC_{last} = 3.93 μM•hr and $t_{1/2}$ = 1.24 h) whereas compound **10** was not detectable following a dose of 25 mg/kg (Fig. 4b) This data correlates well with the results of the Caco-2 permeability assay (Fig. 4a) and supports the development of Sol-moieties possessing a phosphonate group given their superior aqueous solubility and by-product profile.

Discussion

These studies demonstrate the wide utility of the Sol-moiety technology to be applied to both preclinical and clinical stage compounds without the need for sophisticated formulation development.

The chemical scope was demonstrated by successfully linking the Sol-moiety building blocks to primary and secondary amides, sulfonamides, alcohols, amines, anilines, and NH-containing heterocycles as shown in Fig. 3. In general, the carbonyl linkage was used for many Sol-moiety drug-conjugates as this creates a good leaving group to enable the 1,4-elimination reaction to proceed. However, for ease of chemical synthesis and stability under standard acidic deprotection conditions, several prototypes were linked directly to the Sol-moiety via a sulfonamide or amine (**3ii** and **7ii**). In addition, we have shown that Sol-moiety prodrugs can be rapidly evaluated in vitro using the Caco-2 assay, confirming cleavage occurs at the apical side of the cell membrane and allows only the released drug to cross to the basolateral chamber. In all experiments, the charged Sol-moiety-drug conjugate was never observed in the basolateral chamber, only the released

https://doi.org/10.1038/s41467-024-52793-6

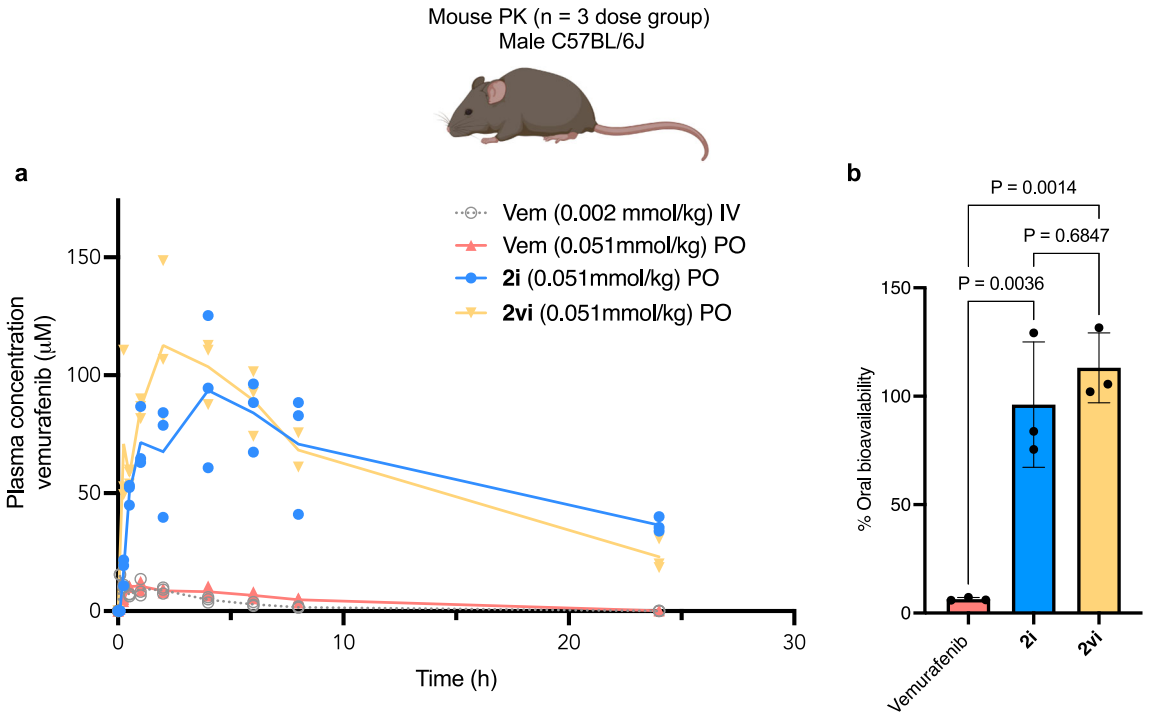

	Vemurafenib		2i	2vi
Dose (mg/kg)	1	25	41[a]	45[a]
Dose (mmol/kg)	0.002	0.051	0.051	0.051
Formulation	5% DMSO, 5% solutol and 90% saline	20% PEG 400, 5% VitE	Saline	Saline
Route of administration	I.V.	Oral	Oral	Oral
Cmax (μM)	15.51	11.2	96.35	122
Tmax (hr)	0.08	0.66	5.33	1.42
$t_{1/2}$ (hr)	2.82	3.35	19.6	9.14
AUC (μM•hr)	50.13	81.02	1200	1418

[a] Dosed at 25 mg/kg equivalent of vemurafenib.

Fig. 7 | Comparison of pharmacokinetic profiles of vemurafenib and Sol-vemurafenib 2i and 2vi. a Plasma concentrations of vemurafenib were measured over 24 h following IV and PO dose of vemurafenib (Vem) in a lipid-based vehicle. Sol-vemurafenib analogs **2i** and **2vi** were dosed via oral gavage in saline solution. $n = 3$ mice per dose group. Line data represents mean values at each time point. **b** Bar chart displaying oral bioavailability of vemurafenib using a 20% PEG 400 based formulation compared to delivery with Sol-vemurafenib **2i** and **2vi** dosed via oral gavage in saline solution. $n = 3$ mice per dose group. Data are presented as mean values +/− SD. Statistical significance was determined using an ordinary one-way ANOVA with Tukey's multiple comparison test. Mouse image Created in BioRender. Smith, M. (2024) BioRender.com/y69d862.

parent drug. These data were confirmed by PK studies that observed only pharmacologically active drug in mouse plasma and no Sol-moiety-linked drug. Furthermore, we confirmed that the major Sol-moiety by-product **10**, possessing the phosphonate group, showed no permeability in the Caco-2 assay and was below the quantifiable limit of detection in plasma following oral delivery in a mouse PK experiment.

The ability of Sol-moiety to improve the oral bioavailability of existing drugs was illustrated using enzalutamide, vemurafenib, and paclitaxel as examples. Enzalutamide is classified as a BCS Class II molecule and is practically insoluble in water (< 0.1 μg/mL) through a range of pH's. As a result, it is administered to patients in either a soft-gel capsule, solvated in caprylocaproyl macroglycerides (CCMG), and dosed as 4 × 40 mg QD[35,36] or in a film-coated tablet using an amorphous form of the drug with cellulosic enhancing polymer[37]. Sol-enzalutamide **1i** was dosed in water and found to have superior oral bioavailability (64%) to the standard CMC/Tween 80-based formulation of enzalutamide (45%). One of the major challenges in developing insoluble drugs is a lack of proportional drug exposure. In contrast to enzalutamide, Sol-enzalutamide **1i** displayed a dose proportional increase in exposure on going from 10 to 50 mg/kg. Furthermore, a boost in oral bioavailability to >80% was observed with the *ortho*-methyl Sol-enzalutamide **1iii**, which we attribute to steric effects slowing the rate of drug release. Additional studies in non-rodent species with long residence time in the intestine would be needed to confirm these observations.

Having optimized oral bioavailability in a BCS Class II molecule, we chose to investigate the oral bioavailability of the BCS class IV drug, vemurafenib. Currently, vemurafenib is administered to melanoma patients with the BRAF mutation using a dosing regimen of 960 mg (4 × 240 mg) twice a day. The drug is formulated as a spray-dried amorphous polymer dispersion with hydroxypropyl methyl cellulose (HPMC) film-coated tablets[38] and suffers from large interpatient variability in pharmacokinetics[39]. However, we demonstrated high oral bioavailability in mice when Sol-vemurafenib was administered by oral gavage using a saline solution as a vehicle, which was >10-fold higher than what was achieved using a PEG-based formulation of the parent drug. The impressive PK profile observed by the Sol-vemurafenib analogs tested would have the potential to reduce pill burden, dosing frequency, and patient PK variability and ultimately improve clinical outcomes.

Finally, to challenge the capacity of the Sol-moiety technology to improve oral PK profiles, we chose to investigate the highly insoluble tubulin inhibitor, paclitaxel. Due to its poor aqueous solubility, low permeability, and first-pass clearance, the oral bioavailability of paclitaxel has been previously measured at <6%[40,41]. Currently, paclitaxel is administered via intravenous infusion over multiple hours once every 3 weeks, using either a Cremophor® EL and ethanol vehicle, or combined with human serum albumin as a suspension infusion. Unfortunately, Cremophor® EL, a pegylated form of castor oil, is known to cause anaphylactic reactions and hypersensitivity in patients and requires pretreatment with steroids for tolerability[42]. Though attempts have been made to develop water-soluble prodrugs of paclitaxel[32,43–46], efforts were mainly focused on replacing Cremophor® EL but either failed to readily release paclitaxel when administered intravenously or displayed no improvement in oral bioavailability. Groups attempting to administer paclitaxel orally with lipid nanoparticles or lipid-based formulation reported that a co-dose with either a P-gp or CYP3A4 inhibitor was necessary to increase absorption and reduce first-pass metabolism[34,47–50]. In contrast, the Sol-moiety prodrug achieved a 5–7-fold improvement in paclitaxel oral bioavailability relative to previously published paclitaxel[40,41] or paclitaxel prodrugs[32,46] without the need for a co-dosed PK enhancer to protect against first past clearance. The significant improvement in drug absorption for **8vi** could be due to a combination of the high solubility observed (> 49 mg/mL pH 6.5) and the rate of hydrolysis by intestinal alkaline phosphatases. Given this exciting result, we chose to run an efficacy study using a BxPC-3 subcutaneous xenograft mouse model. Sol-paclitaxel **8vi**, dosed at 75 mg/kg in saline solution via oral gavage QOD, provided superior efficacy compared to paclitaxel dosed at 12.5 mg/kg IV QWK in a Cremophor® EL-based formulation. The prospect of an oral delivery of paclitaxel could be transformative for patients in terms of efficacy, tolerability, convenience, lowering treatment costs, and health equity.

Though non-rodent pharmacokinetic and toxicological studies are needed to realize the full potential of the Sol-moiety technology, the data presented here clearly demonstrate how the technology can enhance the oral bioavailability of highly insoluble small molecule therapeutics, without the need for sophisticated formulation strategies. Sol-moiety, is a simple solution to an old problem!

Methods

General

Animal work performed in this manuscript complies with the Stanford University Institutional Animal Care and Use Committee regulations and procedures were approved by the Stanford University administrative panel on laboratory animal care or were maintained at UF Scripps or at Rincon Bio in accordance with their regulations on animal laboratory care.

Chemical reactions were performed under ambient atmosphere unless otherwise noted. Qualitative TLC analysis was performed on 250 mm thick, 60 G, glass-backed, F254 silica (EMD Millipore). All solvents used were ACS grade Sure-Seal, and all other reagents were used as received unless otherwise noted. Chromatography was performed on a Biotage Selekt instrument using either Biotage Sfär silica HC columns or Biotage Sfär C-18 HP Sphere 25 μm pre-packed cartridges. Compounds were stored in a freezer (−20 °C) following synthesis. Structure determination was performed using ^{1}H, ^{13}C, ^{19}F, and ^{31}P spectra that were recorded on a Bruker Neo-500 spectrometer, and low-resolution mass spectra (ESI-MS) that were collected on an Agilent LCMS iQ instrument. Unless stated, all chemical building blocks were purchased from commercial sources or were synthesized according to the protocols included in the Supplementary Information. Final compounds were submitted at a purity of >95% by NMR and LCMS.

General synthesis of Sol-enzalutamides 1i and 1iii–v

LiHMDS 1 M in THF (0.22 g, 1.29 mmol) was added to a stirred solution of the Sol-moiety *p*-nitrophenylcarbonate or chloroformate building block (**14** see Supplementary Fig 1) (1.1 mol. equiv.) and enzalutamide (1 mol. equiv.) in THF (0.05 M) cooled to 5 °C. After stirring for 12 h, the excess base is quenched by the addition of 1 M HCl solution, washed with saturated aq. $NaHCO_3$ solution, brine, dried ($MgSO_4$), and evaporated to dryness under reduced pressure. Chromatography (SiO_2; 10–80% ethyl acetate in hexanes) to isolate the protected intermediate. The protected intermediate is dissolved in dichloromethane (0.2 M) cooled to 0 °C and then treated dropwise with TMSBr (12 mol. equiv.). The reaction is allowed to warm to room temperature over 12 h. The excess TMSBr is quenched with the addition of saturated aq. $NaHCO_3$ solution and then evaporated to dryness under reduced pressure. Chromatography (C-18; 30–40% acetonitrile in water) followed by lyophilization provides the desired products **1i, 1iii-v** as sodium salts.

Synthesis of 3-((((4-(3-(4-Cyano-3-(trifluoromethyl)phenyl)-5,5-dimethyl-4-oxo-2-thioxoimidazolidin-1-yl)-2-fluorobenzoyl)(methyl)carbamoyl)oxy)methyl)-4-(phosphonooxy)benzoic acid sodium salt (Sol-enzalutamide 1i)

^{1}H NMR (500 MHz, D_2O) δ 7.69 (d, J = 8.2 Hz, 1H), 7.57 (s, 1H), 7.43 (d, J = 10.5 Hz, 1H), 7.28–7.18 (m, 2H), 7.12 (s, 1H), 6.86 (d, J = 8.7 Hz, 1H), 6.79–6.76 (m, 2H), 4.79 (s, 2H), 2.92 (s, 3H), 0.91 (s, 6H). ^{13}C NMR (125 MHz, methanol-d_4) δ 181.60, 176.63, 174.87, 168.81, 159.91 (d, J = 250.2 Hz), 155.72 (d, J = 5.8 Hz), 155.56, 139.87 (d, J = 10.2 Hz), 139.45, 136.80, 134.50, 133.85 (q, J = 33.1 Hz), 131.57, 130.98 (d, J = 4.0 Hz), 130.52, 128.92 (q, J = 4.7 Hz), 128.42 (d, J = 15.9 Hz), 127.28 (d, J = 3.3 Hz), 126.03 (d, J = 6.8 Hz), 123.69 (q, J = 273.8 Hz), 122.70, 120.04 (d, J = 2.1 Hz), 118.61 (d, J = 23.8 Hz), 116.00, 110.76 (d, J = 2.4 Hz), 68.09, 66.27, 32.37, 23.73 (2 C). ^{31}P NMR (202 MHz, methanol-d_4) δ −1.34. HRMS (ESI): m/z: $[M + H]^+$ calcd for $C_{30}H_{23}F_4N_4O_{10}PS$, 739.0881; found, 739.0890.

3-((((4-(3-(4-Cyano-3-(trifluoromethyl)phenyl)-5,5-dimethyl-4-oxo-2-thioxoimidazolidin-1-yl)-2-fluorobenzoyl)(methyl)carbamoyl)oxy)methyl)-5-methyl-4-(phosphonooxy)benzoic acid sodium salt (Sol-enzalutamide 1iii)

^{1}H NMR (500 MHz, methanol-d_4) δ 8.15 (s, 1H), 8.14 (d, J = 4.6 Hz, 1H), 7.97 (dd, J = 8.2, 2.1 Hz, 1H), 7.79 (d, J = 2.4 Hz, 1H), 7.69 (br d, J = 2.4 Hz, 1H), 7.66 (t, J = 7.9 Hz, 1H), 7.24 (dd, J = 8.1, 2.0 Hz, 1H), 7.21 (dd, J = 10.4, 1.8 Hz, 1H), 5.47 (s, 2H), 3.43 (s, 3H), 2.43 (s, 3H), 1.46 (s, 6H). ^{13}C NMR (125 MHz, methanol-d_4) δ 181.58, 176.55, 169.90, 168.65, 159.93 (d, J = 250.5 Hz), 155.41, 154.76 (d, J = 8.2 Hz), 140.00 (d, J = 10.2 Hz), 139.38, 136.80, 134.45, 133.85 (q, J = 33.4 Hz), 133.44, 133.32, 130.94, 129.84, 128.88 (d, J = 5.1 Hz), 128.57, 128.34, 128.22, 127.38 (d, J = 22.1 Hz), 123.67 (q, J = 273.0 Hz), 118.68 (d, J = 23.7 Hz), 115.98, 110.79, 67.98, 66.09, 32.39, 23.65 (2 C), 17.61. ^{31}P NMR (202 MHz, methanol-d_4) δ −4.07. HRMS (ESI) calcd $C_{31}H_{25}F_4N_4O_{10}PSNa$ $[M + Na]^+$ 775.0857; found 775.0858.

https://doi.org/10.1038/s41467-024-52793-6

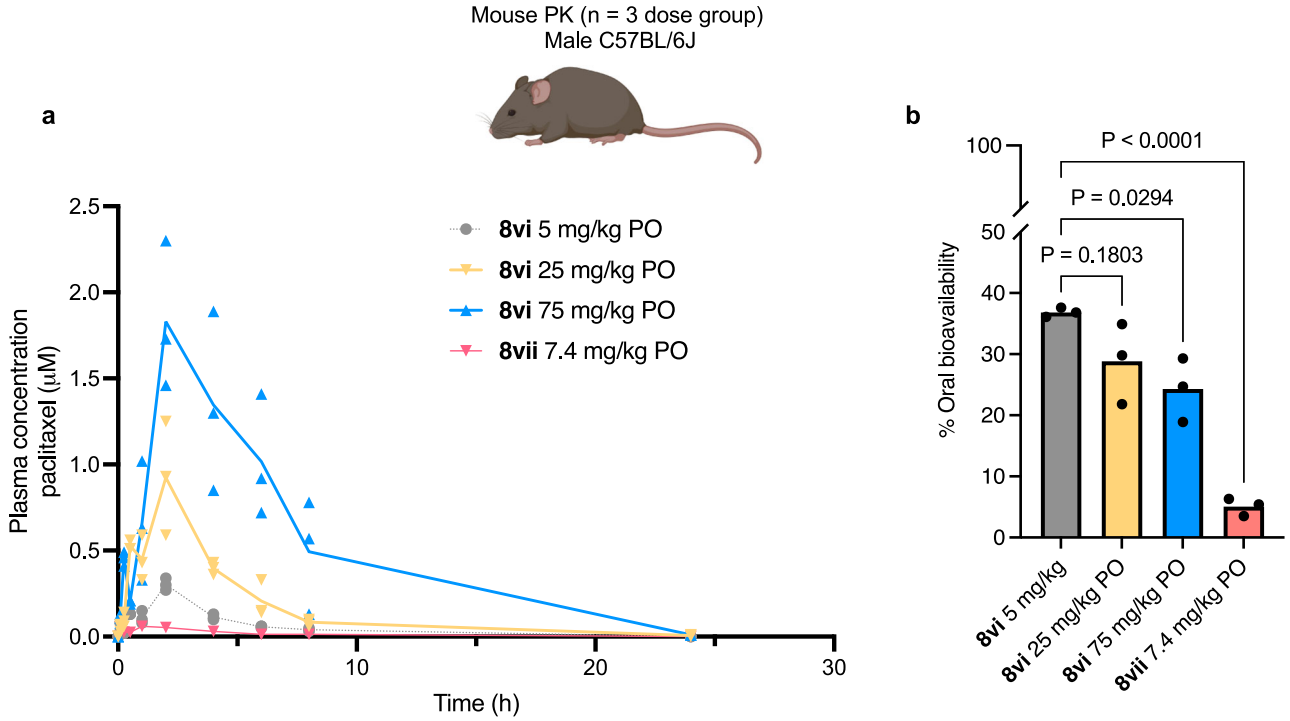

	Paclitaxel	8vii	8vi[a]	8vi	8vi
Dose	1 mg/kg	7.4 kg (6.27 mg/kg of paclitaxel)	5 mg/kg (3.5 mg/kg of paclitaxel)	25 mg/kg (18 mg/kg of paclitaxel)	75 mg/kg (55 mg/kg of paclitaxel)
Dose (mmol/kg)	0.0012	0.0073	0.004	0.021	0.064
Formulation	DMSO (10%), Tween 80 (10%), water (80%)	saline	saline	saline	saline
Route of administration	IV	Oral	Oral	Oral	Oral
Cmax (μM)	0.9	0.06	0.3	0.93	1.83
Tmax (hr)	0.14	1.17	2.0	2.0	2.0
AUC (μM•hr)	0.76 (±0.08)	0.24 (±0.06)	0.98 (±0.02)	3.95 (±0.9)	10.16 (±2.71)

Fig. 8 | Comparison of mouse pharmacokinetic data for paclitaxel. a Plasma concentrations of paclitaxel were measured over 24 h. Paclitaxel was administered intravenously in a DMSO-based formulation whereas the Sol-paclitaxel analogs **8i, 8vi** and the paclitaxel formyl phosphate prodrug **8vii** were all dosed via oral gavage in saline solution. $n = 3$ mice per dose group. Line data represents mean values at each time point. **b** Comparison of oral bioavailability between Sol-paclitaxel **8vi** and paclitaxel possessing a formyl phosphate prodrug **8vii**. $n = 3$ mice per dose group. Data are presented as mean values +/− SD. Statistical significance was determined using an ordinary one-way ANOVA with Tukey's multiple comparison test. Mouse image Created in BioRender. Smith, M. (2024) BioRender.com/y69d862.

3-((((4-(3-(4-Cyano-3-(trifluoromethyl)phenyl)-5,5-dimethyl-4-oxo-2-thioxoimidazolidin-1-yl)-2-fluorobenzoyl)(methyl)carbamoyl)oxy)methyl)-5-fluoro-4-(phosphonooxy)benzoic acid sodium salt (Sol-enzalutamide 1iv)

^{1}H NMR (500 MHz, D_2O) δ 8.14 (d, J = 8.3 Hz, 1H), 8.01 (d, J = 2.0 Hz, 1H), 7.88 (dd, J = 8.3, 2.0 Hz, 1H), 7.67 (t, J = 8.0 Hz, 1H), 7.50 (dd, J = 10.9, 2.1 Hz, 1H), 7.42 (s, 1H), 7.26–7.15 (m, 2H), 5.30 (s, 2H), 3.37 (s, 3H), 1.37 (s, 6H). ^{13}C NMR (125 MHz, acetonitrile-d_3) δ 180.04, 176.41, 172.49, 168.15, 157.96 (d, J = 251.2 Hz), 154.53, 153.91 (d, J = 245.3 Hz), 141.55, 137.57 (d, J = 10.2 Hz), 136.77, 135.95, 132.74, 132.56 (q, J = 32.2 Hz), 131.83, 129.66, 129.13, 127.16, 126.09 (d, J = 14.7 Hz), 125.68, 123.67, 121.59 (d, J = 272.9 Hz), 116.99 (d, J = 23.2 Hz), 116.50 (d, J = 19.7 Hz), 115.16, 109.23, 67.25, 64.39, 31.68, 21.89 (2 C). ^{31}P NMR (202 MHz, acetonitrile-d_3) δ −2.35. HRMS (ESI) calcd for $C_{30}H_{22}F_5N_4O_{10}PSNa$ [M + Na]$^+$ 779.0607; found 779.0608.

3-[[[4-[3-[4-Cyano-3-(trifluoromethyl)phenyl]-5,5-dimethyl-4-oxo-2-thioxo-imidazolidin-1-yl]-2-fluoro-benzoyl]-methyl-carbamoyl]oxymethyl]-5-methoxy-4-phosphonatooxy-benzoate sodium salt (Sol-enzalutamide 1 v)

^{1}H NMR (500 MHz, D_2O) δ 8.14 (d, J = 8.2 Hz, 1H), 8.01 (d, J = 2.3 Hz, 1H), 7.87 (dd, J = 8.2, 2.1 Hz, 1H), 7.68 (d, J = 7.8 Hz, 1H), 7.36 (d, J = 2.3 Hz, 1H), 7.21 (d, J = 2.1 Hz, 1H), 7.19–7.14 (m, 2H), 5.34 (s, 2H), 3.76 (s, 3H), 3.38 (s, 3H), 1.32 (s, 6H). ^{13}C NMR (125 MHz, D_2O) δ 180.52, 177.09, 173.99, 168.91, 158.43 (d, J = 251.5 Hz), 155.08, 151.16, 142.15 (d, J = 7.3 Hz), 137.85 (d, J = 8.9 Hz), 136.85, 136.29, 133.42 (q, J = 32.3 Hz), 132.98, 132.24, 130.15, 127.78, 127.48, 126.37 (d, J = 14.6 Hz), 125.95, 121.91 (q, J = 272.7 Hz), 120.71, 117.35 (d, J = 23.8 Hz), 115.74, 113.12, 109.82, 67.69, 65.16, 55.75, 32.14, 22.13 (2 C). ^{31}P NMR (202 MHz, D_2O) δ 0.35. HRMS (ESI) calcd for $C_{31}H_{25}F_4N_4O_{11}PS$ [M + H]$^+$ 769.0986; found 769.0989.

https://doi.org/10.1038/s41467-024-52793-6

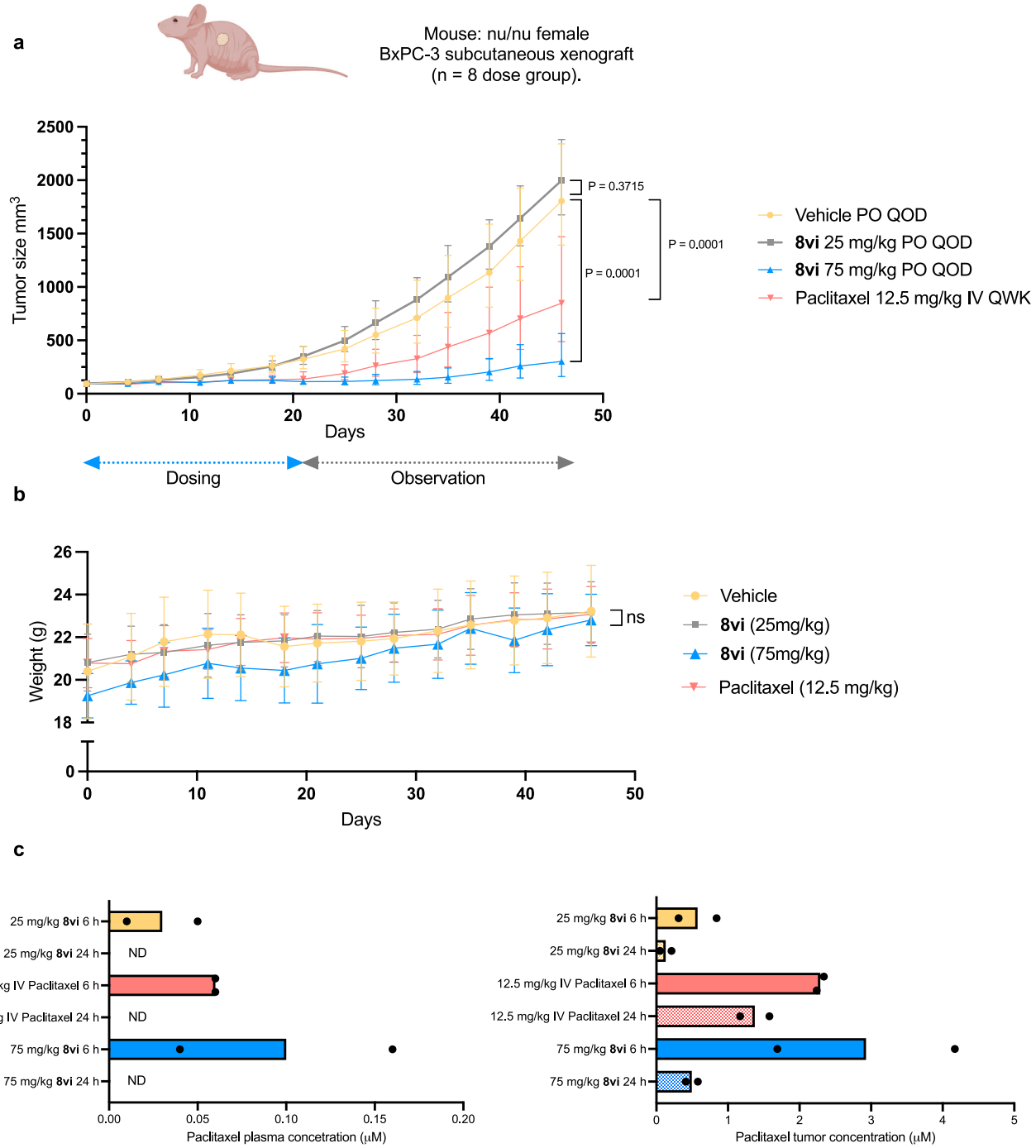

Fig. 9 | Efficacy study using pancreatic BxPC−3 xenograft mouse model. **a** Comparison of paclitaxel administered intravenously once a week (QWK) at a dose of 12.5 mg/kg formulated in Cremophor® EL, ethanol and saline solution and Sol-paclitaxel **8vi** dosed orally once every other day (QOD) at 25 mg/kg and 75 mg/kg (18 mg/kg and 55 mg/kg equivalent of paclitaxel dose respectively) formulated in saline solution. Drug was administered over 21-day period and then monitored for an additional 25 days with tumor volume measured twice a week. $n = 8$ mice per dose group. Data are presented as mean values +/− SD. Statistical significance was determined using an ordinary two-way ANOVA with Dunnett's multiple comparison test. **b** Mouse weight plotted for the duration of the efficacy study (46 days). $n = 8$ mice per dose group. Data are presented as mean values +/− SD. ns = $P > 0.05$ when comparing treatment groups to vehicle. Statistical significance was determined using a mixed-effects analysis with Dunnett's multiple comparison test. **c** Plasma and tumor concentrations of paclitaxel 6 and 24 h post-dose for each dose group. $n = 2$ mice per dose group. The bar chart shows individual and mean values. ND = not detectable. Mouse image created in BioRender. Smith, M. (2024) BioRender.com/d91z968.

Synthesis of (3-(((5-(4-chlorophenyl)-3-(2,6-difluoro-3-(propylsulfonamido)benzoyl)-1*H*-pyrrolo[2,3-*b*]pyridine-1-carbonyl)oxy)methyl)-4-(phosphonooxy)phenyl)phosphonic acid (Sol-vemurafenib 2i)

DIPEA (0.55 mL, 3.06 mmol) was added to a stirred solution of vemurafenib (500 mg, 1.02 mmol), *tert*-butyl 4-diethoxyphosphoryloxy-3-[(4-nitrophenoxy)carbonyloxymethyl]benzoate (600 mg, 1.12 mmol), and DMAP (12 mg, 0.014 mmol) in anhydrous THF (1.0 mL). The reaction mixture was heated at 55 °C for 15 h and then cooled to room temperature and diluted with water. The organic phase was extracted with ethyl acetate, washed with brine, dried ($MgSO_4$) and evaporated to dryness under reduced pressure. Chromatography (SiO_2; 50–70% ethyl acetate in hexanes) provided (5-*tert*-butoxycarbonyl-2-diethoxyphosphoryloxy-phenyl)methyl 5-(4-chlorophenyl)-3-[2,6-difluoro-3-(propylsulfonylamino)benzoyl]pyrrolo[2,3-b]pyridine-1-carboxylate (338 mg, 37%). ^{1}H NMR (500 MHz, $CDCl_3$) δ 8.89 (d, *J* = 2.3 Hz, 1H), 8.64 (d, *J* = 2.3 Hz, 1H), 7.93 (d, *J* = 7.4 Hz, 2H), 7.64–7.58 (m, 2H), 7.57–7.48 (m, 2H), 7.46 (d, *J* = 8.4 Hz, 2H), 7.42–7.38 (m, 1H), 7.08 (t, *J* = 8.4 Hz, 1H), 5.35–5.27 (m, 2H), 4.29–4.16 (m, 4H), 1.93 (m, 2H), 1.56 (s, 9H), 1.40–1.31 (m, 6H), 1.26 (t, *J* = 7.1 Hz, 2H), 1.06 (t, *J* = 7.4 Hz, 3H).

TMSBr (0.78 mL, 4.53 mmol) was added to a stirred solution of (5-*tert*-butoxycarbonyl-2-diethoxyphosphoryloxy-phenyl) methyl 5-(4-chlorophenyl)-3-[2,6-difluoro-3-(propylsulfonylamino)benzoyl]pyrrolo[2,3-b]pyridine-1-carboxylate (900 mg, 0.62 mmol) in dichloromethane (10 mL). The resulting mixture was allowed to stir for 76 h and then the excess TMSBr was quenched by the addition of saturated aq. $NaHCO_3$ solution. The aqueous phase was separated and evaporated to dryness under reduced pressure. Chromatography (C-18; 5–25% acetonitrile in water) followed by lyophilization provided the desired product **2i** (238 mg, 50%) as a white powder. ^{1}H NMR (500 MHz, D_2O) δ 8.56 (d, *J* = 2.1 Hz, 1H), 7.94–7.86 (m, 4H), 7.58 (d, *J* = 9.3 Hz, 1H), 7.55–7.51 (m, 2H), 7.46–7.34 (m, 4H), 5.58 (s, 2H), 4.08–3.87 (m, 2H), 2.07–1.92 (m, 2H), 1.14 (t, *J* = 7.5 Hz, 3H).^{13}C NMR (125 MHz, methanol-d_4) δ 182.11, 175.05, 161.03 (dd, *J* = 253.7, 7.0 Hz), 157.08 (d, *J* = 5.8 Hz), 156.57 (dd, *J* = 252.0, 8.7 Hz), 153.66, 150.51, 144.74, 141.00, 139.78, 138.80, 134.87 (d, *J* = 9.9 Hz), 134.74, 133.19, 132.42, 132.00, 130.22 (2 C), 129.91 (2 C), 129.44, 125.19 (d, *J* = 6.7 Hz), 121.38 (dd, *J* = 15.0, 4.0 Hz), 120.26 (d, *J* = 2.5 Hz), 119.69, 119.46 (dd, *J* = 23.1, 23.1 Hz), 116.99, 113.61 (dd, *J* = 22.9, 3.5 Hz), 66.37, 56.82, 17.99, 13.11. ^{31}P NMR (202 MHz, D_2O) δ −0.26. HRMS (ESI) calcd for $C_{32}H_{25}ClF_2N_3O_{11}PS$ $[M - H]^-$ 762.0531; found 762.0525.

(3-(((5-(4-Chlorophenyl)-3-(2,6-difluoro-3-(propylsulfonamido)benzoyl)-1*H*-pyrrolo[2,3-*b*]pyridine-1-carbonyl)oxy)methyl)-4-(phosphonooxy)phenyl)phosphonic acid (Sol-vemurafenib 2vi)

Was synthesized according to the same procedure as **2i**. ^{1}H NMR (500 MHz, D_2O) δ 8.39 (s, 1H), 7.69 (s, 1H), 7.66–7.59 (m, 1H), 7.59–7.45 (m, 3H), 7.41 (d, *J* = 8.5 Hz, 2H), 7.35–7.24 (m, 3H), 7.15 (t, *J* = 8.6 Hz, 1H), 5.36 (d, *J* = 11.4 Hz, 1H), 5.30 (d, *J* = 11.7 Hz, 1H), 3.77 (m, *J* = 14.8, 7.9 Hz, 1H), 3.67 (m, *J* = 14.8, 7.7 Hz, 1H), 1.83–1.73 (m, 2H), 0.91 (t, *J* = 7.4 Hz, 3H). ^{13}C NMR (125 MHz, methanol-d_4) δ 182.15, 160.67 (dd, *J* = 253.6, 7.5 Hz), 156.49 (dd, *J* = 252.1, 9.0 Hz), 156.35 (dd, *J* = 5.7, 3.4 Hz), 153.83, 150.88, 144.66, 141.23, 138.83, 134.89 (d, *J* = 20.3 Hz), 134.89, 134.71, 134.33 (d, *J* = 9.6 Hz), 133.45, 132.31, 130.22 (2 C), 129.89 (2 C), 129.41, 124.58 (dd, *J* = 13.8, 7.1 Hz), 121.24 (dd, *J* = 15.0, 4.2 Hz), 120.32 (d, *J* = 13.6 Hz), 119.79, 119.40 (t, *J* = 23.5 Hz) 116.88, 113.71 (dd, *J* = 23.2, 4.0 Hz), 67.43, 56.81, 17.93, 13.13. ^{31}P NMR (202 MHz, D_2O) δ 11.84, −0.09. HRMS (ESI) calcd for $C_{31}H_{26}ClF_2N_3O_{12}P_2S$ $[M + H]^+$ 800.0442; found, 800.0429.

Synthesis of 3-[[3-[5-(2-aminopyrimidin-4-yl)-2-*tert*-butyl-thiazol-4-yl]-*N*-(2,6-difluorophenyl)sulfonyl-2-fluoro-anilino]methyl]-4-phosphonatooxy-benzoate sodium salt (Sol-dabrafenib 3ii)

A mixture containing *N*-[3-[5-(2-aminopyrimidin-4-yl)-2-*tert*-butyl-thiazol-4-yl]-2-fluoro-phenyl]-2,6-difluoro-benzenesulfonamide (170 mg, 0.33 mmol), *tert*-butyl 3-(bromomethyl)-4-diethoxyphosphoryloxy-benzoate (138 mg, 0.33 mmol), and Cs_2CO_3 (0.21 mg, 0.66 mmol) in DMSO (3 mL) was stirred at room temperature for 2 h. The reaction material was transferred to a separatory funnel with ethyl acetate and diluted with water. The organic phase was separated, washed with water, brine solution, dried (Na_2SO_4) and then evaporated to dryness under reduced pressure. Chromatography (SiO_2; 20–60% ethyl acetate in hexanes) followed by additional chromatography (C-18; 0–100% acetonitrile in water) afforded *tert*-butyl 3-[[3-[5-(2-aminopyrimidin-4-yl)-2-*tert*-butyl-thiazol-4-yl]-*N*-(2,6-difluorophenyl)sulfonyl-2-fluoro-anilino]methyl]-4-diethoxyphosphoryloxy-benzoate (149 mg, 53%). ^{1}H NMR (500 MHz, $CDCl_3$) δ 8.10 (t, *J* = 1.7 Hz, 1H), 8.05 (d, *J* = 5.3 Hz, 1H), 7.87 (dd, *J* = 8.6, 2.2 Hz, 1H), 7.51–7.41 (m, 2H), 7.41–7.32 (m, 2H), 7.14 (t, *J* = 7.9 Hz, 1H), 6.94 (t, *J* = 8.9 Hz, 2H), 6.17 (d, *J* = 5.3 Hz, 1H), 5.07 (d, *J* = 11.7 Hz, 4H), 4.24–4.14 (m, 4H), 1.54 (s, 9H), 1.44 (s, 9H), 1.29 (td, *J* = 7.0, 1.1 Hz, 6H). *Tert*-butyl 3-[[3-[5-(2-aminopyrimidin-4-yl)-2-*tert*-butyl-thiazol-4-yl]-*N*-(2,6-difluorophenyl)sulfonyl-2-fluoro-anilino]methyl]-4-diethoxyphosphoryloxy-benzoate (149 mg, 0.17 mmol) is dissolved in dichloromethane (3 mL) and treated with TMSBr (0.29 mL, 0.66 mmol). After stirring at room temperature for 72 h, the solvent was evaporated under reduced pressure. The crude residue was treated with saturated aq. $NaHCO_3$ solution (1 mL) to quench the excess TMSBr. The resulting suspension purified by chromatography (C-18; 0–20% acetonitrile in water) followed by lyophilization to give the desired product **3ii** (95 mg, 67%) as a white solid. ^{1}H NMR (500 MHz, D_2O) δ 8.00 (d, *J* = 5.4 Hz, 1H), 7.90 (s, 1H), 7.73–7.61 (m, 3H), 7.53–7.47 (m, 1H), 7.35–7.27 (m, 2H), 7.13 (t, *J* = 9.0 Hz, 2H), 6.12 (d, *J* = 5.5 Hz, 1H), 5.08 (s, 2H), 1.48 (s, 9H). ^{13}C NMR (125 MHz, methanol-d_4) δ 182.67, 174.07, 163.08, 159.76 (dd, *J* = 258.8, 3.9 Hz, 2 C), 158.69, 158.58, 157.07 (d, *J* = 255.5 Hz), 155.12 (d, *J* = 5.6 Hz), 146.08, 135.28 (t, *J* = 11.1 Hz), 134.05, 133.39, 131.66 (d, *J* = 2.7 Hz), 130.08, 129.86, 129.40, 126.67 (d, *J* = 12.4 Hz), 124.38–124.18 (m, 2 C), 118.11 (d, *J* = 2.8 Hz), 116.84 (t, *J* = 16.4 Hz), 112.97 (dd, *J* = 24.0, 3.5 Hz, 2 C), 106.59, 89.71, 49.80, 37.59, 29.59 (3 C). ^{31}P NMR (202 MHz, D_2O) δ −0.34. HRMS (ESI) calcd for $C_{31}H_{27}F_3N_5O_8PS_2$ $[M + H]^+$ 750.1063; found, 750.1065.

Synthesis of 3-((((1-(4-methoxyphenyl)-7-oxo-6-(4-(2-oxopiperidin-1-yl)phenyl)-4,5,6,7-tetrahydro-1*H*-pyrazolo[3,4-*c*]pyridine-3-carbonyl)carbamoyl)oxy)methyl)-4-(phosphonooxy)benzoic acid (Sol-apixaban 4i)

Sodium hydride 60% in mineral oil (31 mg, 0.783 mmol) was added slowly to a stirred solution of apixaban (300 mg, 0.652 mmol) in DMF (3.3 mL) cooled to 0 °C. After 5 min, a solution of *tert*-butyl 4-diethoxyphosphoryloxy-3-[(4-nitrophenoxy)carbonyloxymethyl] benzoate (412 mg, 0.783 mmol) in DMF (1.0 mL) was added and the resulting mixture allowed to gradually warm to ambient temperature and stirred for 12 h. The excess sodium hydride was quenched by the addition of water and the organic phase extracted into ethyl acetate, washed with brine, dried ($MgSO_4$) and evaporated to dryness under reduced pressure. Chromatography (SiO_2; 0–10% methanol in dichloromethane) provided *tert*-butyl 4-diethoxyphosphoryloxy-3-[[1-(4-methoxyphenyl)-7-oxo-6-[4-(2-oxo-1-piperidyl)phenyl]-4,5-dihydropyrazolo[3,4-c]pyridine-3-carbonyl]carbamoyloxymethyl]benzoate (140 mg, 25%). ^{1}H NMR (500 MHz, $CDCl_3$) δ 9.08 (s, 1H), 8.10 (d, *J* = 1.8 Hz, 1H), 7.97 (dd, *J* = 8.6, 2.2 Hz, 1H), 7.47 (dd, *J* = 11.3, 8.7 Hz, 3H), 7.33 (d, *J* = 8.8 Hz, 2H), 7.25 (s, 1H), 6.93 (d, *J* = 9.0 Hz, 2H), 5.37 (s, 2H), 4.24 (ddd, *J* = 8.3, 7.0, 3.3 Hz, 4H), 4.12 (t, *J* = 6.7 Hz, 2H), 3.82 (s, 3H), 3.60

(s, 2H), 3.38 (t, *J* = 6.7 Hz, 2H), 2.60–2.51 (m, 2H), 1.93 (t, *J* = 3.4 Hz, 4H), 1.59 (s, 9H), 1.34 (td, *J* = 7.1, 1.0 Hz, 6H). TMSBr (0.3 mL, 1.62 mmol) was added dropwise to a cooled (0 °C) solution of *tert*-butyl 4-diethoxyphosphoryloxy-3-[[1-(4-methoxyphenyl)-7-oxo-6-[4-(2-oxo-1-piperidyl)phenyl]-4,5-dihydropyrazolo[3,4-c]pyridine-3-carbonyl]carbamoyloxymethyl]benzoate (137 mg, 0.162 mmol) in dichloromethane (3.3 mL). After 12 h, the excess TMSBr was quenched by the addition of saturated aq. $NaHCO_3$ solution. The aqueous phase was separated and evaporated to dryness under reduced pressure. Chromatography (C-18; 0–50% acetonitrile in water) followed by lyophilization provided the desired product **4i** (17 mg, 14%) as a white powder. ^{1}H NMR (500 MHz, D_2O) δ 7.95 (d, *J* = 2.9 Hz, 1H), 7.85 (dd, *J* = 8.5, 2.3 Hz, 1H), 7.53–7.46 (m, 3H), 7.39 (d, *J* = 8.7 Hz, 2H), 7.29 (d, *J* = 8.7 Hz, 2H), 7.05 (d, *J* = 9.0 Hz, 2H), 5.42 (s, 2H), 4.13 (t, *J* = 6.8 Hz, 2H), 3.86 (s, 3H), 3.65–3.59 (m, 2H), 3.28 (t, *J* = 6.8 Hz, 2H), 2.52 (t, *J* = 6.1 Hz, 2H), 1.95–1.88 (m, 4H). (125 MHz, D_2O)) δ 175.66, 174.83, 162.46, 160.19, 159.26, 155.51 (d, *J* = 6.2 Hz), 153.19, 141.85, 140.98, 140.53, 133.84, 132.75, 131.38, 131.15, 130.59, 128.66, 128.00 (2 C), 127.85 (2 C), 127.24 (2 C), 126.22 (d, *J* = 6.2 Hz), 119.83 (d, *J* = 2.9 Hz), 114.67 (2 C), 64.50, 56.28, 52.87, 52.06, 32.26, 22.97, 21.09, 20.81. ^{31}P NMR (202 MHz, D_2O) δ −0.38. HRMS (ESI) calcd for $C_{34}H_{32}N_5O_{12}P$ $[M-H]^-$ 732.1712; found 732.1705.

Synthesis of 4-((((3-((9*H*-carbazol-4-yl)oxy)-2-hydroxypropyl)(2-(2-methoxyphenoxy)ethyl)carbamoyl)oxy)methyl)-3-(phosphonooxy)benzoic acid (Sol-carvedilol 5i)

DIPEA (0.14 mL, 0.78 mmol) was slowly added to a solution of carvedilol (157 mg, 0.39 mmol) and benzyl 3-(chlorocarbonyloxymethyl)-4-dibenzyloxyphosphoryloxy-benzoate (248 mg, 0.43 mmol) in anhydrous THF (1.5 mL). The reaction mixture was allowed to stir at ambient temperature for 1 h and then extracted into ethyl acetate, washed with saturated aq. $NaHCO_3$ solution, 1 M HCl solution, brine, dried (Na_2SO_4) and then evaporated to dryness under reduced pressure. Chromatography (SiO_2; 20–70% ethyl acetate in hexanes) provided benzyl 3-[[[3-(9H-carbazol-4-yloxy)-2-hydroxy-propyl]-[2-(2-methoxyphenoxy)ethyl]carbamoyl]oxymethyl]-4-dibenzyloxyphosphoryloxy-benzoate (249 mg, 64%) as a colorless oil that was solvated in ethanol (10 mL) and treated with 10% wet Pd/C (75 mg). The mixture was placed under an atmosphere of hydrogen and stirred rapidly for 1 h, flushed with nitrogen and then filtered through Celite®, rinsed with methanol and evaporated to dryness under reduced pressure. Chromatography (C-18; 20–70% acetonitrile in water) followed by lyophilization provided the desired product **5i** (140 mg, 75%) as white powder. ^{1}H NMR (500 MHz, D_2O at 80 °C) δ 8.78 (br s, 1H), 8.41 (br s, 2H), 8.11 (br s, 1H), 8.06 (br s, 1H), 8.00 (br s, 1H), 7.95 (br s, 1H), 7.75 (br s, 2H), 7.39 (br s, 2H), 7.31 (br s, 3H), 5.83 (br s, 2H), 5.04 (br s, 1H), 4.88 (br s, 2H), 4.75 (br s, 2H), 4.31 (br s, 4H), 4.15 (br s, 3H). ^{13}C NMR (125 MHz, methanol-d_4) δ 175.52, 158.87 (d, *J* = 38.4 Hz), 156.54, 150.92, 149.60, 142.91, 140.66, 131.60, 131.30, 130.86, 127.44, 127.38, 125.51, 124.20, 123.57, 122.60 (d, *J* = 17.6 Hz), 122.13, 120.05, 119.86, 115.05 (d, *J* = 15.8 Hz), 113.63, 113.41, 113.28, 110.90, 104.93, 101.51, 71.15*, 69.76*, 68.86*, 64.92, 56.36, 53.29*, 49.79 (*split peaks due to rotamers). ^{31}P NMR (202 MHz, D_2O) δ −0.30. HRMS (ESI) calcd for $C_{33}H_{33}N_2O_{12}PNa$ $[M + Na]^+$ 703.1663; found 703.1670.

Synthesis of 3-[[[3-(9H-carbazol-4-yloxy)-2-hydroxy-propyl]-[2-(2-methoxyphenoxy)ethyl]carbamoyl]oxymethyl]-4-phosphonooxy-benzoic acid sodium salt (Sol-lenalidomide 6i)

Tert-butyl 3-(chlorocarbonyloxymethyl)-4-diethoxyphosphoryloxy-benzoate (896 mg, 2.12 mmol) was added to a solution of lenalidomide (500 mg, 11.92 mmol) and DIPEA (1.0 mL, 15.78 mmol) in THF (5.0 mL). The reaction solution was stirred at 80 °C for 16 h and then allowed to cool to room temperature and diluted with water (30 mL), The organic phase was extracted with ethyl acetate, washed with brine, dried (Na_2SO_4) and evaporated to dryness under reduced pressure. Chromatography (SiO_2; 0–10% methanol in dichloromethane) provided *tert*-butyl 4-diethoxyphosphoryloxy-3-[[2-(2,6-dioxo-3-piperidyl)-1-oxo-isoindolin-4-yl]carbamoyloxymethyl]benzoate (503 mg, 66%) as a yellow oil. ^{1}H NMR (500 MHz, $CDCl_3$) δ 9.05–9.00 (m, 1H), 8.07 (t, *J* = 1.6 Hz, 1H), 8.05–7.96 (m, 1H), 7.92 (td, *J* = 8.3, 2.3 Hz, 1H), 7.72 (d, *J* = 8.0 Hz, 1H), 7.52 (dd, *J* = 7.5, 0.9 Hz, 1H), 7.40–7.32 (m, 2H), 5.28 (s, 2H), 4.66 (d, *J* = 8.4 Hz, 1H), 4.43–4.27 (m, 2H), 4.27–4.17 (m, 4H), 1.56 (d, *J* = 5.3 Hz, 4H), 1.55 (s, 9H), 1.33 (dtt, *J* = 14.1, 7.0, 1.2 Hz, 6H). TMSBr (0.81 mL, 4.33 mmol) was added to a cooled (0 °C) solution of *tert*-butyl 4-diethoxyphosphoryloxy-3-[[2-(2,6-dioxo-3-piperidyl)-1-oxo-isoindolin-4-yl]carbamoyloxymethyl]benzoate (850 mg, 1.31 mmol) in anhydrous dichloromethane (12.4 mL). The reaction solution was allowed to gradually warm to ambient temperature, heated at 45 °C for 18 h and then allowed to cool to room temperature. Excess TMSBr was quenched with saturated aq. $NaHCO_3$ solution and then evaporated to dryness under reduced pressure. Chromatography (C-18; 0–75% acetonitrile in water) followed by lyophilization provided **6i** as an off-white solid (671 mg, 91%). ^{1}H NMR (500 MHz, D_2O) δ 7.94 (d, *J* = 2.6 Hz, 1H), 7.84 (dd, *J* = 8.6, 2.4 Hz, 1H), 7.73 (d, *J* = 7.9 Hz, 1H), 7.65–7.60 (m, 1H), 7.58–7.53 (m, 1H), 7.49 (d, *J* = 8.5 Hz, 1H), 5.37 (s, 2H), 5.11 (dd, *J* = 13.4, 5.3 Hz, 1H), 4.48 (d, *J* = 17.5 Hz, 1H), 4.41 (d, *J* = 17.5 Hz, 1H), 2.94–2.84 (m, 2H), 2.50–2.41 (m, 1H), 2.29–2.18 (m, 1H). ^{13}C NMR (125 MHz, DMSO-d_6) δ 172.83, 170.97, 167.79, 167.21, 156.65, 153.84, 133.94, 133.19, 132.79, 129.97, 129.83, 128.73, 126.47, 124.36, 123.28, 119.79, 118.43, 61.80, 51.62, 46.42, 31.19 and 22.53. ^{31}P NMR (202 MHz, DMSO-d_6) δ −5.28. HRMS (ESI) calcd for $C_{22}H_{20}N_3O_{11}PNa$ $[M + Na]^+$ 556.0728; found 556.0736.

Synthesis of 3-[[4-(13-chloro-4-azatricyclo[9.4.0.03,8]pentadeca-1(15),3(8),4,6,11,13-hexaen-2-ylidene)-1-piperidyl]methyl]-4-phosphonooxy-benzoic acid sodium salt (Sol-desloratadine 7ii)

DIPEA (0.084 mL, 0.48 mmol) was added to a solution of desloratadine (124 mg, 0.4 mmol) and *tert*-butyl 3-(bromomethyl)-4-diethoxyphosphoryloxy-benzoate (169 mg, 0.4 mmol) in dichloromethane (2 mL). The resulting solution was allowed to stir at room temperature for 12 h and then diluted with dichloromethane, washed with water, saturated aq. NH_4Cl solution, brine, dried ($MgSO_4$) and then evaporated to dryness under reduced pressure. Chromatography (SiO_2; 0–5% methanol in dichloromethane) provided *tert*-butyl 3-[[4-(13-chloro-4-azatricyclo[9.4.0.03,8]pentadeca-1(15),3(8),4,6,11,13-hexaen−2-ylidene)-1-piperidyl]methyl]−4-diethoxyphosphoryloxy-benzoate (120 mg, 46%) as tan oil. ^{1}H NMR (500 MHz, methanol-d_4) δ 8.30 (dd, *J* = 4.9, 1.6 Hz, 1H), 8.10 (s, 1H), 7.89 (dd, *J* = 8.6, 2.2 Hz, 1H), 7.68–7.62 (m, 1H), 7.37 (dd, *J* = 8.7, 1.0 Hz, 1H), 7.24 (dd, *J* = 7.7, 4.9 Hz, 1H), 7.21 (d, *J* = 2.1 Hz, 1H), 7.16 (dd, *J* = 8.2, 2.2 Hz, 1H), 7.11 (d, *J* = 8.2 Hz, 1H), 4.33–4.20 (m, 4H), 3.62 (s, 2H), 3.45–3.35 (m, 2H), 2.92–2.82 (m, 2H), 2.81–2.75 (m, 2H), 2.53–2.41 (m, 2H), 2.37 (dt, *J* = 13.9, 4.5 Hz, 1H), 2.31–2.19 (m, 3H), 1.59 (s, 9H), 1.34 (td, *J* = 7.1, 1.1 Hz, 6H). TMSBr (0.32 ml) was added to a solution of *tert*-butyl 3-[[4-(13-chloro-4-azatricyclo[9.4.0.03,8]pentadeca-1(15),3(8),4,6,11,13-hexaen-2-ylidene)-1-piperidyl]methyl]-4-diethoxyphosphoryloxy-benzoate (110 mg, 0.17 mmol) in dichloromethane (1.5 mL) at room temperature. (1.5 mL) and then TMSBr (0.32 ml). After stirring for 24 h, solid $NaHCO_3$ (200 mg, 2.38 mmol) was added to the reaction mixture and the solvent removed under reduced pressure. Chromatography (C-18; 0–60% acetonitrile in water) followed by lyophilization provided **7ii** (58 mg, 64%) as an off-white solid. ^{1}H NMR (500 MHz, methanol-d_4) δ 8.36 (d, *J* = 4.9 Hz, 1H), 8.12 (dd, *J* = 8.6, 1.8 Hz, 2H), 7.67 (dd, *J* = 7.8, 1.5 Hz, 1H), 7.45 (d, *J* = 8.5 Hz, 1H), 7.28 (dd, *J* = 7.8, 4.9 Hz, 1H), 7.26 (d, *J* = 2.0 Hz, 1H), 7.21 (dd, *J* = 8.2, 2.1 Hz, 1H), 7.16 (d, *J* = 8.5 Hz, 1H), 4.32 (s, 2H), 3.39 (br s, 6H), 2.97–2.79 (m, 2H),

2.76–2.63 (m, 2H), 2.45 (br s, 2H). ^{13}C NMR (125 MHz, methanol-d_4) δ 168.63, 157.54 (d, J = 7.4 Hz), 157.33, 147.27, 141.40, 139.98, 137.87, 136.83, 136.00, 135.93, 134.72, 134.38, 133.80, 131.31, 130.45, 128.57, 127.35, 124.64, 124.51, 124.15, 56.63, 53.59, 53.55, 32.38, 31.97, 28.76, 28.55. ^{31}P NMR (202 MHz, methanol-d_4) δ −3.62. HRMS (ESI) calcd for $C_{27}H_{26}ClN_2O_6PNa$ [M + Na]$^+$ 563.1109; found 563.1104.

Synthesis of 3-((((((1*S*,2 *R*)-1-benzamido-3-(((2a*R*,4*S*,4a*S*,6 *R*,9*S*,11*S*,12*S*,12a*R*,12b*S*)-6,12b-diacetoxy-12-(benzoyloxy)-4,11-dihydroxy-4a,8,13,13-tetramethyl-5-oxo-2a,3,4,4a,5,6,9,10,11,12,12a,12b-dodecahydro-1*H*-7,11-methanocyclodeca[3,4]benzo[1,2-*b*]oxet-9-yl)oxy)-3-oxo-1-phenylpropan−2-yl)oxy)carbonyl)oxy)methyl)-4-(phosphonooxy)benzoic acid (Sol-paclitaxel 8i)

A solution of benzyl 3-(chlorocarbonyloxymethyl)-4-dibenzyloxyphosphoryloxy-benzoate (636 mg, 1.10 mmol) in dichloromethane (3.0 mL) was added to stirred solution of paclitaxel (850 mg, 0.99 mmol) and DIPEA (0.35 mL, 1.99 mmol) in dichloromethane cooled to 0 °C. The reaction was allowed to gradually warm to ambient temperature over 6 h and then diluted with water. The organic phase was extracted with dichloromethane, washed with brine, dried ($MgSO_4$) and evaporated to dryness under reduced pressure. Chromatography (SiO_2; ethyl acetate in hexanes) provided benzyl 3-[[(1 R)-1-[(S)-benzamido(phenyl)methyl]-2-[[(1S,2S,4S,7 R,9S,10S,12 R,15S)-4,12-diacetoxy-2-benzoyloxy-1,9-dihydroxy-10,14,17,17-tetramethyl-11-oxo-6-oxatetracyclo[11.3.1.03,10.04,7]heptadec-13-en-15-yl]oxy]-2-oxo-ethoxy]carbonyloxymethyl]-4-dibenzyloxyphosphoryloxy-benzoate (975 mg, 70%) as a colorless foam. The product was dissolved in ethanol (13 mL) and treated with 5% Pd/C (~5 mg) and the reaction vessel evacuated and placed under atmosphere of hydrogen and stirred vigorously for 45 min. The reaction vessel was evacuated, flushed with nitrogen gas and then filtered through GF/F paper, washed with ethanol and evaporated to dryness under reduced pressure. Chromatography (C-18; 50% methanol in water) followed by lyophilization provided the desired product **8i** (141 g, 18%). ^{1}H NMR (500 MHz, methanol-d_4) δ 8.11 (d, J = 7.6 Hz, 2H), 8.06 (s, 1H), 7.96 (d, J = 7.9 Hz, 1H), 7.81 (d, J = 7.5 Hz, 2H), 7.71–7.66 (m, 1H), 7.59–7.54 (m, 3H), 7.54–7.49 (m, 3H), 7.47–7.40 (m, 4H), 7.33–7.27 (m,1H), 6.45 (s, 1H), 6.10 (t, J = 9.2 Hz, 1H), 5.85 (d, J = 6.3 Hz, 1H), 5.64 (d, J = 7.2 Hz, 1H), 5.52 (d, J = 6.3 Hz, 1H), 5.44 (d, J = 13.3 Hz, 1H), 5.36 (d, J = 13.0 Hz, 1H), 5.00 (d, J = 9.6 Hz, 1H), 4.35 (dd, J = 11.0, 6.6 Hz, 1H), 4.19 (s, 2H), 3.82 (d, J = 7.2 Hz, 1H), 2.53–2.44 (m, 1H), 2.41 (s, 3H), 2.22 (dd, J = 15.4, 9.5 Hz, 1H), 2.18 (s, 3H), 1.91 (s, 3H), 1.89–1.76 (m, 2H), 1.65 (s, 3H), 1.14 (s, 6H).^{13}C NMR (125 MHz, methanol-d_4) δ 205.24, 171.66, 171.29, 170.64, 170.21, 169.21, 167.69, 156.31 (d, J = 3.1 Hz), 155.71, 142.34, 138.22, 135.46, 134.85, 132.84, 132.33, 131.72, 131.40, 131.20 (2 C), 130.09 (2 C), 129.71 (2 C), 129.65, 129.55 (2 C), 128.67 (2 C), 128.63 (2 C), 127.78 (d, J = 4.6 Hz), 126.60, 120.97, 120.48, 85.96, 82.24, 79.02, 78.58, 77.47, 76.82, 76.28, 73.21, 72.27, 66.68, 59.20, 55.38, 47.87, 44.59, 37.53, 36.46, 26.95, 23.22, 22.41, 20.78, 14.95, 10.46. ^{31}P NMR (202 MHz, methanol-d_4) δ −4.98. HRMS (ESI) calcd for $C_{56}H_{58}NO_{22}P$ [M + H]$^+$ calcd 1128.3261; found, 1128.3252.

Synthesis of (3-((((((1*S*,2 *R*)-1-benzamido-3-(((2a*R*,4*S*,4a*S*,6 *R*,9*S*,11*S*,12*S*,12a*R*,12b*S*)-6,12b-diacetoxy-12-(benzoyloxy)-4,11-dihydroxy-4^a,8,13,13-tetramethyl−5-oxo-2^a,3,4,4^a,5,6,9,10,11,12,12^a,12b-dodecahydro-1*H*-7,11-methanocyclodeca[3,4]benzo[1,2-*b*]oxet-9-yl)oxy)-3-oxo-1-phenylpropan-2-yl)oxy)carbonyl)oxy)methyl)-4-(phosphonooxy)phenyl)phosphonic acid (Sol-paclitaxel 8vi)

A solution of (5-dibenzyloxyphosphoryl-2-dibenzyloxyphosphoryloxy-phenyl)methyl carbonochloridate (910 mg, 1.29 mmol) in dichloromethane (2 mL) was added to a cooled (0 °C) solution of paclitaxel (1.0 g, 1.17 mmol) and DIPEA (0.41 mL, 2.34 mmol) in dichloromethane (4 mL). After stirring for 5 h, the reaction mixture was diluted with water, extracted into dichloromethane, washed with brine solution, dried ($MgSO_4$), and evaporated to dryness under reduced pressure. Chromatography (SiO_2; 10–80% ethyl acetate in hexanes) provided the protected intermediate. This material was dissolved in ethanol (8.6 mL) and treated with 10% Pd/C (cat.). The reaction mixture was placed under an atmosphere of hydrogen and stirred vigorously for 40 min. The reaction vessel was evacuated, flushed with nitrogen, filtered through GF/F paper, washed with ethanol, and evaporated to dryness under reduced pressure. The residue was dissolved in water and washed several times with 2-MeTHF to remove excess paclitaxel. The aqueous layer was evaporated to dryness under reduced pressure. Chromatography (C-18; 50% methanol in water) provided the desired product **8vi** (978 mg, 54%) as a white solid. ^{1}H NMR (500 MHz, methanol-d_4) δ 8.17–8.11 (m, 2H), 7.94 (d, J = 13.4 Hz, 1H), 7.86–7.77 (m, 3H), 7.72–7.65 (m, 1H), 7.62–7.56 (m, 2H), 7.54–7.49 (m, 4H), 7.48–7.41 (m, 4H), 7.29–7.26 (m, 1H), 6.48 (s, 1H), 6.13 (t, J = 8.4 Hz, 1H), 5.87 (d, J = 6.1 Hz, 1H), 5.67 (d, J = 7.3 Hz, 1H), 5.53 (d, J = 6.1 Hz, 1H), 5.43 (d, J = 12.8 Hz, 1H), 5.36 (d, J = 12.8 Hz, 1H), 5.02 (dd, J = 9.7, 2.4 Hz, 1H), 4.37 (dd, J = 11.1, 6.6 Hz, 1H), 4.21 (s, 2H), 3.84 (d, J = 7.2 Hz, 1H), 2.50 (ddd, J = 14.3, 9.7, 6.6 Hz, 1H), 2.43 (s, 3H), 2.23 (dd, J = 15.6, 9.6 Hz, 1H), 2.19 (s, 3H), 1.97 (d, J = 1.5 Hz, 3H), 1.89 (dd, J = 15.3, 9.1 Hz, 1H), 1.83 (ddd, J = 14.3, 11.1, 2.4 Hz, 1H), 1.68 (s, 3H), 1.17 (s, 3H), 1.16 (s, 3H). ^{13}C NMR (125 MHz, methanol-d_4) δ 205.16, 171.65, 171.30, 170.58, 170.20, 167.65, 155.65, 153.49 (dd, J = 6.5, 3.7 Hz), 142.29, 138.11, 135.38, 134.89, 134.61, 133.84 (d, J = 11.0 Hz), 133.58 (d, J = 11.8 Hz), 132.88, 131.36, 131.19 (2 C), 130.38, 130.12 (2 C), 129.71 (2 C), 129.56 (2 C), 128.87, 128.62 (2 C), 128.57 (2 C), 128.06 (dd, J = 15.6, 6.6 Hz), 121.19 (dd, J = 15.8, 2.8 Hz), 85.88, 82.26, 79.01, 78.59, 77.45, 76.81, 76.23, 73.21, 72.31, 66.27, 59.21, 55.31, 47.86, 44.57, 37.48, 36.41, 26.93, 23.24, 22.39, 20.78, 14.95, 10.45. ^{31}P NMR (202 MHz, methanol-d_4) δ 14.78, −5.76. HRMS (ESI) calcd for $C_{55}H_{59}NO_{23}P_2Na$ [M + Na]$^+$ 1186.2845; found 1186.2843.

Caco-2 permeability assays

Was performed using a similar procedure as outlined by Hidalgo[51]. Caco-2 cells were purchased from ATCC (HTB-37) and maintained in DMEM containing 10% FBS in an incubator at 37 °C of 5% CO_2. 50,000 cells/well were seeded on 12-well plate with polycarbonate filter inserts (Millipore Corporation, CLS3401) and allowed to grow and differentiate for 25 ± 4 days in DMEM containing 10% FBS before the cell monolayers were used for experiments. Test articles and reference compounds (propranolol, atenolol, enzalutamide, vemurafenib, dabrafenib, apixaban, carvedilol, lenalidomide, desloratadine and paclitaxel) were dissolved in DMSO before further dissolved in HBSS (Millipore Corporation, H1387-10X1L) containing 25 mM HEPES to yield a final concentration of 10 mM. The assays were performed in HBSS at pH 7.4 for the basolateral side and pH 6.5 for apical side at 37 °C. Prior to the study, the monolayers were washed in prewarmed HBSS. At the start of the experiments, pre-warmed HBSS containing the test articles was added to the apical side of the monolayer and HBSS, without test articles, was added to the basolateral side. Aliquots from the basolateral chamber were taken over the 2 h incubation period; aliquots of the apical side were taken at 0 h and 2 h. All donor wells (apical chambers) contained 100 mM lucifer yellow to monitor for tight junction integrity. Sample aliquots were diluted with an equal volume of methanol/water with 0.1% formic acid containing the internal standard. The mixture was analyzed by LCMS/MS to monitor concentration of both the Sol-moiety-drug conjugate as well as the released parent. The apparent permeability coefficients (Papp) were calculated using the formula: Papp = $(dC_{rec}/dt)/(A \times C_{0,donor})] \times 10^6$.

In vivo pharmacokinetics

Male C57BL/6 mice were administered the Sol-moiety drug prototypes by oral gavage (18/22-gauge gavage needle with a rounded ball at the tip to prevent injury during insertion), directly into the stomach using

saline solution (0.9% NaCl) or deionized water as a vehicle (dose of 10 µL/g body weight). Microbleeds via the tail vein at indicated time points over 24 h were performed on each mouse.

IV injections were made using a 27/29- or 30-gauge insulin syringe, and the dose was injected into the right or left lateral tail vein or via the retro-orbital route. IV injection of paclitaxel was dosed at a concentration of 0.2 mg/ml (5 µL/g body weight) using a formulation consisting of DMSO (10%), Tween 80 (10%), and water (80%). Enzalutamide and vemurafenib were formulated in DMSO (10%) and water (90%). Mice were maintained and experiments were performed at UF Scripps Institute for Biomedical Innovation & Technology or at Stanford University. Mice were randomly assigned to each dose group and the researchers performing the dosing. Mice were housed in either Optimice carousel sterile quarters with filtered air supply in disposable cages from Animal Care Systems, Inc. (Centennial, CO) or housed on Innovive IVC mouse racks with filtered air supplied in recyclable Innocage mouse cages form Innovive (San Diego, CA). A 12-hour light/12-hour dark light cycle is observed, with animal handling only taking place during the light cycle. Parent drug concentration was analyzed by LC-MS/MS. *P* values were determined using an ordinary One Way ANOVA in GraphPad Prism.

In vivo efficacy studies using pancreatic cancer xenograft mouse tumor model

Female Foxn nu/nu mice (4 weeks old at time of delivery) were procured through Jackson laboratory. Mice were housed in Optimice carousel sterile quarters with filtered air supply in disposable cages from Animal Care Systems, Inc. (Centennial, CO). A 12-hour light/12-hour dark light cycle is observed, with animal handling only taking place during the light cycle. On the day of implantation, BxPC-3 cells were trypsinized and allowed to detach from flasks. Trypsin was then neutralized with complete media and cells were spun at 400 x *g*. Media was aspirated and cells were resuspended in 50:50 *Cultrex BME, Type 3:DMEM (no supplementation) at a concentration of 3.5×10^7 cells/mL. A volume of 100 µL was injected into the right hind flank of each animal (a total of 3.5×10^6 cells).

When mean tumor volume reached ~95 mm^3, mice were stratified and randomly placed into four treatment groups of eight mice for the efficacy study and four treatment groups of four mice for the plasma and tumor PK study. Treatments were administered by oral gavage (20-gauge 38 mm flexible nylon) or by tail vein injection (adjusted by mouse weight for 10 mL/kg dosing). The PK mice were dosed with a single dose. Tumor volumes were measured by digital caliper by the same technician each time and volume was calculated using the formula [$Width^2 \times$ Length]/2. Tumor volumes were analyzed in Prism 10.1.1 (GraphPad) using a mixed model and a Dunnett post hoc analysis for repeated measures with multiple comparisons. The maximal tumor size was 3000 mm^3 and was not exceeded during the study. Mice were maintained and experiments were conducted at RinconBio, Utah. Plasma and tumor concentrations of paclitaxel were analyzed at UF Scripps Institute for Biomedical Innovation & Technology. Data analysis was performed using independent experimental samples.

Reporting summary

Further information on research design is available in the Nature Portfolio Reporting Summary linked to this article.

Data availability

Chemical synthesis of intermediates and spectral data for compounds tested in the animal efficacy studies, along with protocols and data for the solubility, stability, and alkaline phosphatase hydrolysis assays are included in the supplementary information document (PDF). Source data for the mouse PK and PD experiments (Figs. 4–9) are provided with the manuscript. Source data are provided with this paper.

References

1. Schaadt, R., Sweeney, D., Shinabarger, D. & Zurenko, G. In vitro activity of TR-700, the active ingredient of the antibacterial prodrug TR-701, a novel oxazolidinone antibacterial agent. *Antimicrob. Agents Chemother.* **53**, 3236–3239 (2009).
2. Meanwell, N. A. et al. Inhibitors of HIV-1 attachment: The discovery and development of temsavir and its prodrug fostemsavir. *J. Med. Chem.* **61**, 62–80 (2019).
3. Falcoz, C. et al. Pharmacokinetics of GW433908, a prodrug of amprenavir, in healthy male volunteers. *J. Clin. Pharmacol.* **42**, 887–898 (2002).
4. Baloum, M., Grossbard, E. B., Mant, T. & Lau, D. T. W Pharmacokinetics of fostamatinib, a spleen tyrosine kinase (SYK) inhibitor, in healthy human subjects following single and multiple oral dosing in three Phase 1 studies. *Br. J. Clin. Pharmcol.* **76**, 78–88 (2012).
5. Bergenheim, A. T. & Henriksson, R. Pharmacokinetics and pharmacodynamics of estramustine phosphate. *Clin. Pharmacokinet.* **34**, 163–172 (1998).
6. Bodor, N., Harget, A. J. & Phillips, E. W. Structure-activity relationships in the antiinflammatory steroids: a pattern-recognition approach. *J. Med. Chem.* **26**, 318–328 (1983).
7. Ikeda, Y. et al. Stability and stabilization studies of TAK-599 (ceftaroline fosamil), a novel *n*-phosphono type prodrug of anti-methicillin resistant staphylococcus aureus cephalosporin T-91825. *Chem. Pharm. Bull.* **56**, 1406–1411 (2008).
8. Hale, J. J. et al. Phosphorylated morpholine acetal human neurokinin-1 receptor antagonists as water-soluble prodrugs. *J. Med. Chem.* **43**, 1234–1241 (2000).
9. Aapro, M. et al. Netupitant-palonosetron (NEPA) for preventing chemotherapy-induced nausea and vomiting: from clinical trials to daily practice. *Curr. Cancer Drug Targets* **22**, 806–824 (2022).
10. Cooke, A. et al. Water-soluble propofol analogues with intravenous anaesthetic activity. *Bioorg. Med. Chem. Lett.* **11**, 927–930 (2001).
11. Kouvaris, J. R., Kouloulias, V. E. & Vlahos, L. J. Amifostine: The first selective-target and broad-spectrum radioprotector. *Oncologist* **12**, 738–747 (2007).
12. Fields, S. Z. et al. Phase I study of etoposide phosphate (etopophos) as a 30-minute infusion on days 1, 3, and 5. *Clin. Cancer Res.* **1**, 105–111 (1995).
13. Sobue, S., Tan, K. & Haug-Pihale, G. The effects of hepatic impairment on the pharmacokinetics of fosfluconazole and fluconazole following a single intravenous bolus injection of fosfluconazole. *Br. J. Clin. Pharmacol.* **59**, 160–166 (2005).
14. Fischer, J. H., Patel, T. V. & Fischer, P. A. Fosphenytoin: clinical pharmacokinetics and coparative advantages in the acute treatment of seizures. *Clin. Pharmacokinet.* **42**, 33–58 (2003).
15. Casper, E. S., Mittelman, A., Kelson, D. & Young, C. W. Phase I clinical trial of fluarabine phosphate (F-ara-AMP). *Cancer Chemother. Pharmacol.* **15**, 233–235 (1985).
16. Morris, C. A. et al. Review of the clinical pharmacokinetics of artesunate and its active metabolite dihydroartemisinin following intravenous, intramuscular, oral or rectal administration. *Malar. J.* **10**, 263 (2011).
17. Kunimoto, T. et al. Antitumor activity of 7-ethyl-10-[4-(1-piperidino)-1-piperidino]carbonyloxycamptothecin, a novel water-soluble derivative of camptothecin, against murine tumors. *Cancer Res.* **47**, 5944–5947 (1987).
18. Ohwada, J. et al. Design, synthesis and antifungal activity of a novel water soluble prodrug of antifungal triazole. *Bioorg. Med. Chem. Lett.* **13**, 191–196 (2003).
19. Evans, D. F. et al. Measurement of gastrointestinal pH profiles in normal ambulant human subjects. *Gut* **29**, 1035–1041 (1988).

20. Jantzen, J.-P., Tzanova, I., Witton, P. K. & Klein, A. M. Rectal pH in children. *Can. J. Anaesth.* **36**, 665–776 (1989).
21. Heimbach, T. et al. Absorption rate limit considerations for oral phosphate prodrugs. *Pharm. Res.* **20**, 848 (2003).
22. Heimbach, T. et al. Enzyme mediated precipitation of their parent drugs from their phosphate prodrugs. *Int. J. Pharm.* **261**, 81–92 (2003).
23. DeCoey, D. A. et al. Water-soluble prodrugs of the human immunodeficiency virus protease inhibitors lopinavir and ritonavir. *J. Med. Chem.* **52**, 2964–2970 (2009).
24. Mäntylä, A. et al. Design, synthesis and in vitro evaluation of novel water-soluble prodrugs of buparvaquone. *Eur. J. Pharm. Sci.* **23**, 151–158 (2004).
25. Lui, C. et al. Discovery of ((4-(5-(Cyclopropylcarbamoyl)-2-methylphenylamino)- 5-methylpyrrolo[1,2-f][1,2,4]triazine-6- carbonyl) (propyl)carbamoyloxy)methyl–2-(4- (phosphonooxy)phenyl)acetate (BMS-751324), a Clinical Prodrug of p38α MAP Kinase Inhibitor. *J. Med. Chem.* **8**, 7775–7784 (2015).
26. Narvekar, M., Xue, H. Y., Eoh, J. Y. & Wong, H. L. Nanocarrier for poorly water soluble anticancer drugs—barriers of translation. *AAPS PharmSciTech* **15**, 822–833 (2014).
27. Boyd, B. J. et al. Successful oral delivery of poorly water-soluble drugs both depends on the intraluminal behaviour of drugs and of appropriate advanced delivery systems. *Eur. J. Pharm. Sci.* **137**, 104967 (2019).
28. Hann, M. M. & Keseru, G. M. Finding the sweet spot: the role of nature and nurture in medicinal chemistry. *Nat. Rev. Drug Disc.* **11**, 355–365 (2012).
29. Sanchini, S., Perruccio, F. & Piizzi, G. Rational design, synthesis and biological evaluation of modular fluorogenic substrates with high affinity and selectivity for PTP1B. *ChemBioChem* **15**, 961–976 (2014).
30. Pinto, M., Robine-Leon, S. & Appay, M.-D. Enterocyte-like differentiation and polarization of the human colon carcinoma cell line Caco-2 in culture. *Biol. Cell.* **47**, 323–330 (1983).
31. Tran, C. et al. Development of a second-generation antiandrogen for treatment of advanced prostate cancer. *Science* **324**, 787–790 (2009).
32. Golik, J. et al. Synthesis and antitumor evaluation of paclitaxel phosphonooxymethyl ethers: a novel class of water soluble paclitaxel pro-drugs. *Bioorg. Med. Chem.* **6**, 1837–1842 (1996).
33. Stage, T. B., Bergmann, T. K. & Kroetz, D. L. Clinical pharmacokientics of paclitaxel monotherapy: an updated literature review. *Clin. Pharmacokinet.* **57**, 7–19 (2018).
34. Jang, E. et al. DHP23002 as a next generation oral paclitaxel formulation for pancreatic cancer therapy. *PLoS One* **14**, e0225095 (2019).
35. Kim, T.-K. et al. Pharmacokinetics of enzalutamide, an anti-prostate cancer drug, in rats. *Arch. Pharm. Res.* **38**, 2076–2082 (2015).
36. European Medicines Agency CHMP Assessment Report for Xtandi enzalutamide EMA/CHMP/383457/2013.
37. Gelabert, S. F., Fernandez, L. A. & Kumar R. Pharmaceutical composition comprising enzalutamide. WO2021064123.
38. Shah, N. et al. Improved human boavailability of vemurafenib, a practically insoluble drug, using an amorphous polymer-stabilized solid dispersion prepared by a solvent-controlled coprecipitation process. *J. Pharm. Sci.* **102**, 967–981 (2013).
39. Zhang, W., Heinzmann, D. & Grippo, J. F. Clinical pharmacokinetics of vemurafenib. *Clin. Pharmacokinet.* **56**, 1033–1043 (2017).
40. Peltier, S., Oger, J.-M., Lagrace, F., Couet, W. & Benoit, J.-P. Enhanced oral paclitaxel bioavailability after administration of paclitaxel-loaded lipid nanocapsules. *Pharm. Res.* **23**, 1243–1250 (2006).
41. Sparreboom, A. et al. Limited oral bioavailability and active epithelial excretion of paclitaxel (Taxol) caused by P-glycoprotein in the intestine. *Proc. Natl Acad. Sci. USA* **94**, 2031–2035 (1997).
42. Gelderblom, H., Verweij, J., Nooter, K. & Sparreboom, A. Cremophor EL: the drawbacks and advantages of vehicle selection for drug formulation. *Eur. J. Cancer* **37**, 1590–1598 (2001).
43. Vyas, D. M. et al. Synthesis and antitumor evaluation of water soluble taxol phosphates. *Bioorg. Med. Chem.* **3**, 1357–1360 (1993).
44. Ueda, Y. et al. Novel water soluble phosphate prodrugs of taxol possessing in vivo antitumor activity. *Bioorg. Med. Chem.* **3**, 1761–1766 (1993).
45. Ueda, Y. et al. Synthesis and antitumor evaluation of 2′-oxycarbonylpaclitaxels (paclitaxel-2′-carbonates). *Bioorg. Med. Chem.* **4**, 1861–1864 (1994).
46. Gund, M. et al. Water-soluble prodrugs of paclitaxel containing self-immolative disulfide linkers. *Bioorg. Med. Chem. Lett.* **25**, 122–12 (2015).
47. Malingre, M. M., Beijnen, J. H. & Schellens, J. H. M. Oral delivery of taxanes. *Invest. N. Drug* **19**, 155–162 (2001).
48. Chu, Z. et al. Oral bioavailability of a novel paclitaxel formulation (genetaxyl) administered with cyclosporin a in cancer patients. *Anticancer Drugs* **19**, 275–281 (2008).
49. Bardelmeijer, H. A. et al. Increased oral bioavailability of paclitaxel by gf120918 in mice through selective modulation of P-glycoprotein. *Clin. Cancer Res.* **6**, 4416–4421 (2000).
50. Hendrikx, J. J. M. A. et al. Oral co-administration of elacridar and ritonavir enhances plasma levels of oral paclitaxel and docetaxel without affecting relative brain accumulation. *Br. J. Cancer* **110**, 2669–2676 (2014).
51. Hidalgo, I. J., Raub, T. J. & Borchardt, R. T. Characterization of the human colon carcinoma cell line (Caco-2) as a model system for intestinal epithelial permeability. *Gastroenterology* **96**, 736–749 (1989).

Acknowledgements

Additional pharmacokinetic analysis for this publication was performed at UF Scripps Institute for Biomedical Innovation & Technology, under the supervision of Dr. Michael Cameron. This data was collected using a mass spectrometer funded by NIH grant number 1 S10OD030332-01. We would like to thank Dr. Chris Carreras for helpful discussion regarding the alkaline phosphatase assay. Efficacy studies using the BxPC-3 xenograft tumor mouse model were performed at Rincon Bio, Salt Lake City, UT. Several of the pictures used in the manuscript were prepared in BioRender. Funding of this work was kindly provided by Sarafan ChEM-H, Stanford University.

Author contributions

M.S. conceived the project, designed the compounds in this study, and interpreted the data generated. A.B.K., J.D.B., T.C.M., K.A.S., D.C., D.G.D. C.M. and K.K. performed synthetic chemistry. A.H. supervised D.C. and K.K. and provided conceptual advice to the project. A.B.K., J.D.B., T.C.M., and D.A.C. performed analytical chemistry on the final products. R.S., H.X., and J.P.A. performed in vivo pharmacokinetic experiments and interpreted the data. J.P.A. provided data analysis and advice on pharmacokinetic and pharmacodynamic studies. K.C.N. performed the Caco-2 assay. B.B.W. performed the alkaline phosphatase assay and performed data analysis of the results. A.B.K., J.D.B., and T.C.M. performed the solubility and stability assays and performed data analysis of the results. The manuscript was written by M.S. and A.B.K. through contributions of all authors. All authors have given approval to the final version of the manuscript.

Competing interests

The authors declare no competing interests. A provisional patent application has been filed by The Board of Trustees of the Leland Stanford Junior University. Inventor: Mark Smith US 63/600,382. The patent application covers the composition claims over the Sol-moiety drug conjugates and Sol-moiety precursors as well as method claims for

prodrug preparation and use of Sol-moiety as a prodrug for delivery of a medicament.

Additional information

Supplementary information The online version contains supplementary material available at https://doi.org/10.1038/s41467-024-52793-6.

Correspondence and requests for materials should be addressed to Mark Smith.

Peer review information *Nature Communications* thanks Shutao Guo and Jarkko Rautio for their contribution to the peer review of this work. A peer review file is available.